

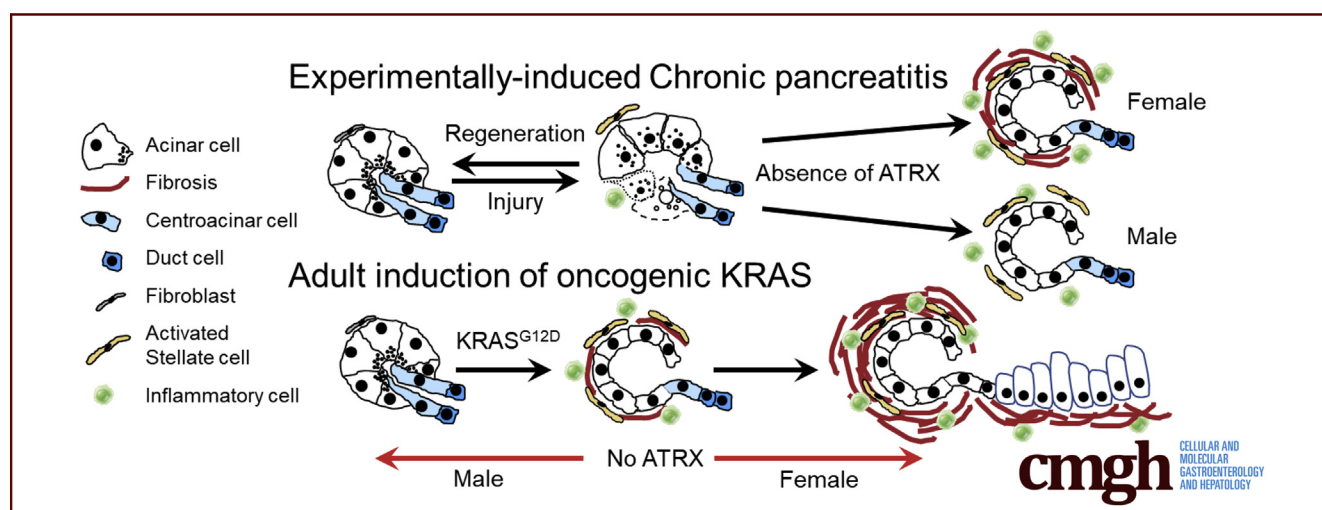
ORIGINAL RESEARCH

The Loss of ATRX Increases Susceptibility to Pancreatic Injury and Oncogenic KRAS in Female But Not Male Mice



Claire C. Young,^{1,2,3,7} Ryan M. Baker,^{1,7} Christopher J. Howlett,⁴ Todd Hryciw,^{5,6} Joshua E. Herman,⁶ Douglas Higgs,⁸ Richard Gibbons,⁸ Howard Crawford,⁹ Arthur Brown,^{5,6,7} and Christopher L. Pin^{1,2,3,7}

¹Department of Paediatrics, ²Department of Physiology and Pharmacology, ³Department of Oncology, ⁴Department of Pathology and Laboratory Medicine, and ⁵Department of Anatomy and Cell Biology, Schulich School of Medicine & Dentistry, University of Western Ontario, ⁶Robarts Research Institute, and ⁷Children's Health Research Institute, London, Ontario, Canada; ⁸MRC Molecular Haematology Unit, Institute of Molecular Medicine, John Radcliffe Hospital, Oxford, United Kingdom; and ⁹Molecular & Integrative Physiology and Internal Medicine, University of Michigan, Ann Arbor, Michigan



SUMMARY

Female mice lacking ATRX in the pancreas have increased sensitivity to pancreatic cancer, whereas male mice without ATRX are protected. This study identifies such susceptibility in pancreatic cancer and highlights the need for sex-specific approaches in cancer treatment.

BACKGROUND: Pancreatic ductal adenocarcinoma (PDAC) is the third leading cause of cancer death in North America, accounting for >30,000 deaths annually. Although somatic activating mutations in KRAS appear in 97% of PDAC patients, additional factors are required to initiate PDAC. Because mutations in genes encoding chromatin remodelling proteins have been implicated in KRAS-mediated PDAC, we investigated whether loss of chromatin remodeler α -thalassemia, mental-retardation, X-linked (ATRX) affects oncogenic KRAS's ability to promote PDAC. ATRX affects DNA replication, repair, and gene expression and is implicated in other cancers including glioblastomas and pancreatic neuroendocrine tumors. The hypothesis was that deletion of *Atrx* in pancreatic acinar cells will increase susceptibility to injury and oncogenic KRAS.

METHODS: Mice allowing conditional loss of *Atrx* within pancreatic acinar cells were examined after induction of recurrent cerulein-induced pancreatitis or oncogenic KRAS ($KRAS^{G12D}$). Histologic, biochemical, and molecular analysis examined pancreatic pathologies up to 2 months after induction of *Atrx* deletion.

RESULTS: Mice lacking *Atrx* showed more progressive damage, inflammation, and acinar-to-duct cell metaplasia in response to injury relative to wild-type mice. In combination with $KRAS^{G12D}$, *Atrx*-deficient acinar cells showed increased fibrosis, inflammation, progression to acinar-to-duct cell metaplasia, and pre-cancerous lesions relative to mice expressing only $KRAS^{G12D}$. This sensitivity appears only in female mice, mimicking a significant prevalence of ATRX mutations in human female PDAC patients.

CONCLUSIONS: Our results indicate the absence of ATRX increases sensitivity to injury and oncogenic KRAS only in female mice. This is an instance of a sex-specific mutation that enhances oncogenic KRAS's ability to promote pancreatic intraepithelial lesion formation. (*Cell Mol Gastroenterol Hepatol* 2019;7:93–113; <https://doi.org/10.1016/j.jcmgh.2018.09.004>)

Keywords: Epigenetics; Pancreatic Ductal Adenocarcinoma; MIST1; SOX9.

Pancreatic ductal adenocarcinoma (PDAC) is the third leading cause of cancer-related death in North America, with a 5-year survival rate of ~9% (Pancreatic Cancer Facts, PANCAN). PDAC is characterized by increased genomic instability,¹ a poor response to chemotherapeutic intervention, and often diagnosed at later stages because of a lack of clinical symptoms and poor diagnostic markers even for susceptible populations. During the last 10 years, elegant lineage tracing studies identified acinar cells as the cell of origin in many PDAC cases.^{2–4} In these cases, the initiating events include acinar-to-duct cell metaplasia (ADM), in which mature acinar cells transiently revert to a pancreatic progenitor-like state, increasing the potential for progression to neoplastic lesions termed pancreatic intraepithelial lesions (PanINs) and PDAC.^{2,5}

Mutations in *KRAS* that lead to a constitutively active form of the protein are a hallmark of PDAC, present in 97% of cases.³ However, the constitutive activation of *KRAS* alone appears to be insufficient to drive PDAC progression, and additional acquired mutations and/or pancreatic injury are required.^{1,6,7} Recent molecular characterization of PDAC tumors has identified 4 subtypes for PDAC and mutations that define 10 pathways commonly affected in these tumors. In addition to identifying RAS and NOTCH signaling as key oncogenic pathways, somatic mutations in genes involved in chromatin remodeling and SWI/SNF function were identified.⁸ Studies using genetically modified mouse strains harboring null alleles for the chromatin remodeling proteins brahma-related gene 1⁹ or B-cell specific Moloney virus insertion site 1¹⁰ increased and decreased, respectively, the ability for oncogenic *KRAS* to promote PDAC progression. These studies confirm the importance of maintaining chromosome organization/integrity in preventing *KRAS*-mediated oncogenic progression. Our goal was to explore the idea that other components that contribute to SWI/SNF function and genome integrity may be functionally linked to oncogenic *KRAS* activity in promoting PDAC.

ATRX (α -thalassemia, mental-retardation, X-linked) is a member of the SWI/SNF family of proteins and interacts with death associated protein 6 (DAXX) to maintain or remodel appropriate nucleosome organization within the genome.^{11,12} In addition to its role in chromatin remodeling, studies have identified roles for ATRX in maintaining genomic stability,¹³ maintaining proper DNA replication and repair,¹⁴ and affecting gene expression.¹⁵ It has been proposed that ATRX-dependent deposition of histone variant H3.3 prevents the formation of alternative DNA structures during replication, allowing for proper facilitation of the replicative process.^{15,16} Complete loss of ATRX function during development is lethal,¹⁷ but hypomorphic *ATRX* mutations are the underlying cause for ATRX syndrome, a developmental disorder in males involving significant cognitive impairment, facial abnormalities, and development of α -thalassemia.¹⁸ More recently, somatic mutations in *ATRX* have been identified in a number of cancers including glioblastomas and pancreatic neuroendocrine tumors.^{19–22}

To date, the role of ATRX in the adult pancreas or PDAC has not been examined. Therefore, we investigated the effect of

ATRX deletion on pancreatic injury and oncogenic *KRAS*-mediated PDAC progression. We generated mouse lines in which exon 18 of the mouse *ATRX* gene could be conditionally deleted in pancreatic acinar cells on its own or in combination with activation of oncogenic *KRAS*. Our results showed that loss of ATRX alters the response to recurrent pancreatic injury, suggesting a role for ATRX in the repair and regeneration of acinar tissue after pancreatic insult. Furthermore, combination of *Atrx* deletion with oncogenic *KRAS* activation significantly enhanced pancreatic damage within 2 months relative to oncogenic *KRAS* alone. Surprisingly, this ability to sensitize the pancreatic acinar cells to the oncogenic action of mutated *KRAS* was observed exclusively in female mice. These results indicate that ATRX loss cooperates with activated *KRAS* to promote pancreatic disease in a sex-specific manner.

Results

To determine whether *ATRX* deletion affected the phenotype of mature acinar cells, *Atrx*^{fl Δ 18} mice²³ were mated to mice expressing *creERT* from the *Mist1* locus (*Mist1*^{creERT}; Figure 1A), allowing for acinar-specific deletion in the pancreas.^{24,25} Deletion of exon 18 results in complete loss of ATRX, likely because of mRNA instability.²³ A shorter isoform of *ATRX* may still be expressed, but this truncated form lacks the SWI/SNF domain.²⁶ Tamoxifen was administered to 2- to 4-month-old mice, and ATRX accumulation was assessed 7, 35, or 60 days after dosing (Figure 1B and C). Immunofluorescence analysis confirmed 98% of acinar cells were ATRX-negative at all time points, demonstrating efficient *Atrx* deletion and indicating mature acinar cells do not require ATRX for maintained viability (Figure 1C). Co-immunofluorescence for ATRX and insulin and identification of duct nuclei based on morphology confirmed *Atrx* deletion specifically in acinar cells (Figure 1D).

Histologic analysis showed no obvious phenotypes regarding disorganization of acinar cells or injury/inflammation (Figure 2A), although intralobular adipocytes were observed at a higher frequency in *Mist1*^{creERT/+} *Atrx*^{fl Δ 18} mice. Because loss of ATRX showed limited effects on overall pancreatic morphology, we focused specifically on the 60-day time point to determine whether any phenotypes occurred in response to loss of ATRX. Immunofluorescence analysis for proliferative markers Ki67 (Figure 2B) and pH3 (data not shown) or TUNEL analysis (Figure 2C) revealed increased numbers of proliferating and apoptotic cells after

Abbreviations used in this paper: ADM, acinar-to-duct cell metaplasia; ANOVA, analysis of variance; ATRX, α -thalassemia, mental-retardation, X-linked; CIP, cerulein induced pancreatitis; CPA, carboxypeptidase; DAXX, death associated protein 6; ds, double stranded; EZH2, Enhancer of Zeste Homologue 2; MKA, *Mist1*^{creERT/+} *Kras*^{LSL-G12D/+} *Atrx*^{fl Δ 18}; PanIN, pancreatic intraepithelial lesion; PDAC, pancreatic ductal adenocarcinoma; WT, wild-type.



Most current article

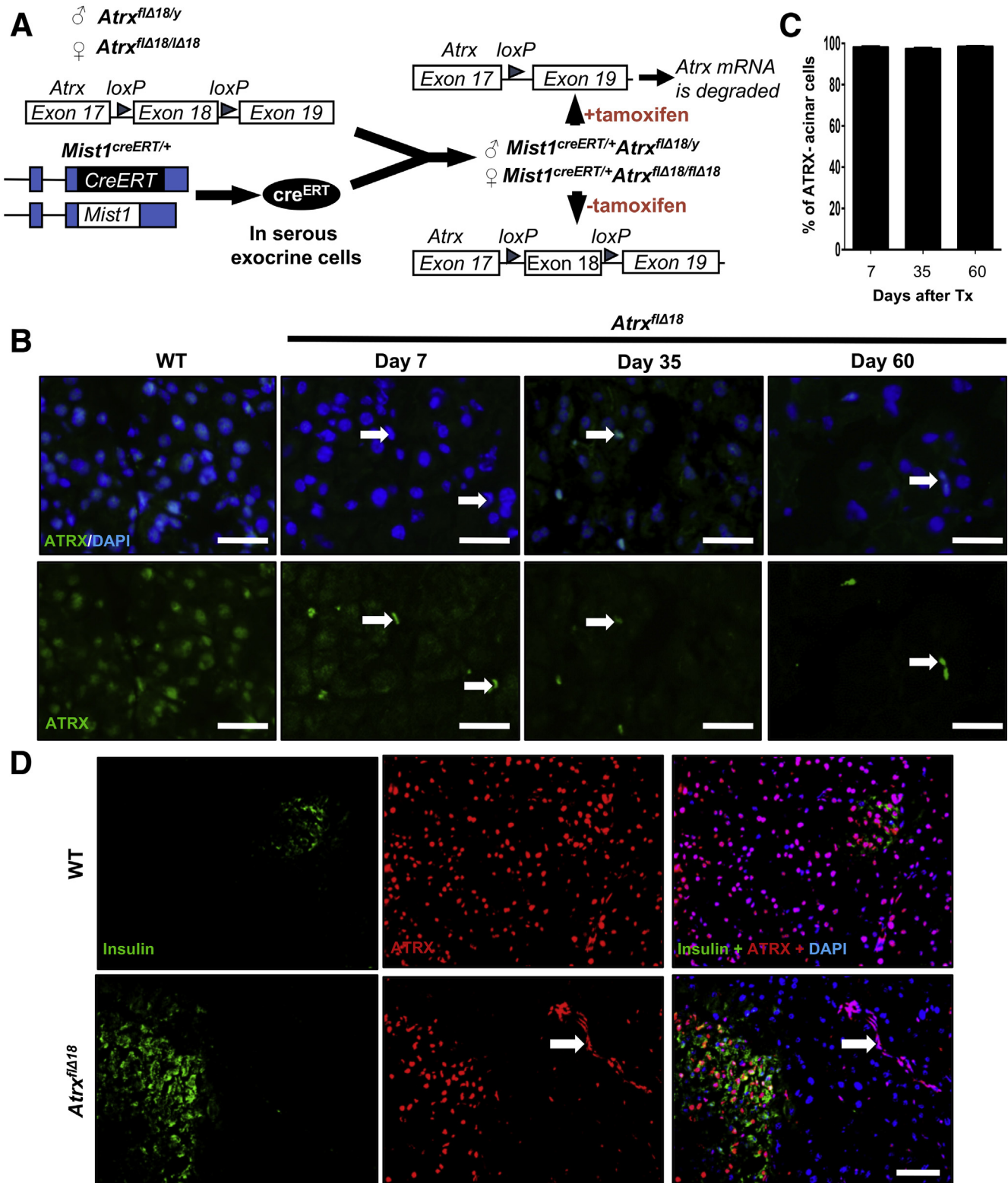
© 2018 The Authors. Published by Elsevier Inc. on behalf of the AGA Institute. This is an open access article under the CC BY-NC-ND license (<http://creativecommons.org/licenses/by-nc-nd/4.0/>).

2352-345X

<https://doi.org/10.1016/j.jcmgh.2018.09.004>

ATRX deletion. Because ATRX is involved in double stranded (ds) DNA repair,^{14,27} we examined γ H2AX accumulation, a marker for unresolved dsDNA breaks. *Mist1*^{creERT/+}*Atrx*^{fl Δ 18} pancreatic tissue showed an increase in the number of cells accumulating γ H2AX (Figure 2D), suggesting loss of ATRX

leads to an inability to resolve dsDNA breaks. These results suggest that short-term loss of ATRX in pancreatic acini has no overt consequences on pancreatic morphology but may increase susceptibility to events that require intact DNA repair pathways, such as pancreatic injury.



To examine this possibility, *Mist1^{creERT/+}* and *Mist1^{creERT/+} Atrx^{flΔ18}* mice were subjected to recurrent pancreatic injury for 11 days and allowed to recover for 3 days. We chose a mild dosing regimen so damage in control mice would be limited. No significant differences were observed between *Mist1^{creERT/+}* and *Mist1^{creERT/+} Atrx^{flΔ18}* mice based on body weight, behavior, or gross tissue morphology 3 days after cessation of cerulein (data not shown). However, histologic analysis showed marked differences between the 2 genotypes in response to cerulein treatment. As expected, cerulein-treated *Mist1^{creERT/+}* mice show intra-acinar edema but no evidence of inflammation or fibrosis (Figure 3A), likely because of the mild nature of the cerulein treatment. Conversely, cerulein-treated *Mist1^{creERT/+} Atrx^{flΔ18}* mice showed increased damage (Figure 3A) and fibrosis in female *Mist1^{creERT/+} Atrx^{flΔ18}* mice relative to controls (Figure 3B and C), as indicated by H&E and trichrome histology, respectively. This enhanced cellular damage was further confirmed by the strong immunofluorescence signal for F4/80 antigen that was indicative of extensive macrophage infiltration in *Mist1^{creERT/+} Atrx^{flΔ18}* mice relative to controls (Figure 3D). Quantification of the tissue damage confirmed increased sensitivity to recurrent cerulein induced pancreatitis (CIP) and indicated that female *Mist1^{creERT/+} Atrx^{flΔ18}* mice are clearly more sensitive than male mice to these effects (Figure 3C, Table 2). Whereas analysis of acinar cell death by cleaved caspase-3 showed no difference between genotypes (Figure 4A), notably enhanced cell turnover based on cleaved caspase-3 (Figure 4B) or proliferative capacity by Ki67 staining (Figure 5E) was observed in *Mist1^{creERT/+} Atrx^{flΔ18}* pancreata in areas showing classic features of ADM after CIP. No such areas of ADM were observed in *Mist1^{creERT/+}* mice (Table 2).

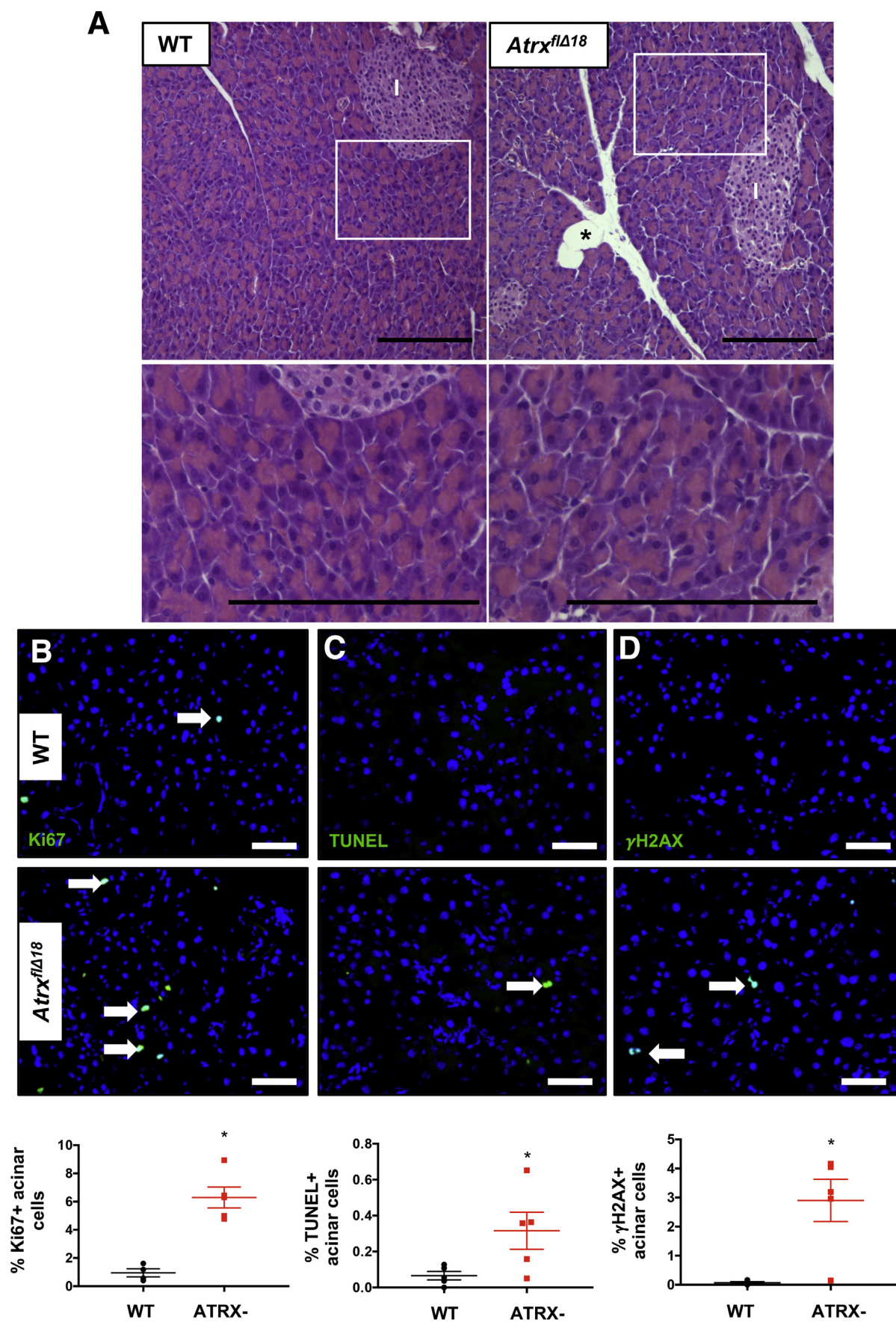
Tissue histology also revealed a notable increase in ADM in *Mist1^{creERT/+} Atrx^{flΔ18}* tissue based on the appearance of tubular complexes (Figure 3B). Western blot analysis (Figure 5A) for mature acinar cell markers amylase and pro-carboxypeptidase (CPA) confirmed a different response to recurrent CIP in *Mist1^{creERT/+} Atrx^{flΔ18}* mice. Cerulein-treated *Mist1^{creERT/+}* mice exhibited increased accumulation of amylase and CPA compared with saline-treated controls, which was indicative of a regenerative response to injury. However, *Mist1^{creERT/+} Atrx^{flΔ18}* mice did not show this recovery from injury (Figure 5A). This difference in enzyme accumulation was not due to increased release of enzymes in response to injury because circulating levels of amylase were not significantly different between genotypes (Figure 5B). Immunohistochemical analysis confirmed

decreased CPA accumulation in both putative ADM as well as surrounding acinar cells (Figure 5C). Surprisingly, this decrease in CPA accumulation appeared to be more dramatic in cerulein-treated female *Mist1^{creERT/+} Atrx^{flΔ18}* mice. Acini (delineated by a dotted line) show limited CPA accumulation in tissue sections from female mice (Figure 5C). We next examined expression of the progenitor/duct cell marker SOX9, a transcription factor that increases during regeneration and is required for ADM.⁴ In adult pancreatic tissue, SOX9 is expressed only in a subset of duct and centroacinar cells,^{4,28} which we confirmed by immunofluorescence on sections from saline-treated and cerulein-treated *Mist1^{creERT/+}* mice (Figure 5D and E). Conversely, increased SOX9 nuclear accumulation was observed in female and male *Mist1^{creERT/+} Atrx^{flΔ18}* pancreatic tissue specifically after CIP treatment (Figure 5D), accumulating in ADM and some acinar cells (Figure 5D and E). Taken together, these data suggest loss of ATRX increased the sensitivity of acinar cells to recurrent cerulein exposure.

These findings suggest that *Mist1^{creERT/+} Atrx^{flΔ18}* mice will have increased susceptibility to oncogenic properties of mutated KRAS, because maintenance of the acinar phenotype constrains KRAS-induced transformation.^{5,9,29} Therefore, we next introduced an inducible form of oncogenic KRAS (*Kras^{LSL-G12D/+}*) into the *Mist1^{creERT/+} Atrx^{flΔ18}* genotype (*Mist1^{creERT/+} Kras^{LSL-G12D/+} Atrx^{flΔ18}* hereafter referred to as *MKA*; Figure 6A). Cre-mediated induction of *KRAS^{G12D}* +/- deletion of *Atrx* was initiated in 2- to 4-month-old congenic *Mist1^{creERT/+}*, *Mist1^{creERT/+} Atrx^{flΔ18}*, *Mist1^{creERT/+} Kras^{LSL-G12D/+}*, and *MKA* mice (Figure 6B), and acinar cell-specific loss of ATRX was confirmed by immunohistochemistry (Figure 6C). No significant differences were observed in body weight between groups during the course of the experiment (Figure 6D), and assessment of serum amylase levels at the time of death revealed no differences between genotypes (Figure 6E). Because of the presence of oral squamous papilloma tumors in *KRAS^{G12D}*-expressing mice, the experiment was terminated at 60 days after tamoxifen administration (data not shown). Gross morphologic examination revealed enlarged spleens in female *Mist1^{creERT/+} Kras^{LSL-G12D/+}* and *MKA* mice (Figure 7).

Histologic examination revealed normal pancreatic morphology in *Mist1^{creERT/+}* and *Mist1^{creERT/+} Atrx^{flΔ18}* mice (Figure 8A). *Mist1^{creERT/+} Kras^{LSL-G12D/+}* mice also showed typical pancreatic morphology for the most part, with a few instances of ADM or PanINs (Figure 8A). This is consistent with previous reports that activation of oncogenic *KRAS^{G12D}* in mature acinar cells was insufficient on its own to cause

Figure 1. (See previous page). Loss of ATRX in the pancreas is specific to acinar cells. (A) Schematic of *Atrx* deficient model. *Atrx^{flΔ18}* mice carrying loxP sites that flank exon 18. *CreERT* is expressed from the *Mist1* promoter. On tamoxifen administration to *Mist1^{creERT/+} Atrx^{flΔ18}* mice, *cre* recombinase becomes localized to the nucleus and produces deletion of exon 18 of the *Atrx* gene. This leads to degradation of full-length *Atrx* mRNA. (B) Immunofluorescence for ATRX in pancreatic tissue from *Mist1^{creERT/+}* (WT) mice 7, 35, or 60 days after tamoxifen gavage in *Mist1^{creERT/+} Atrx^{flΔ18}* mice (*Atrx^{flΔ18}*). White arrows indicate residual ATRX expression. Magnification bars = 25 μm. (C) *Atrx* deletion efficiency was quantified as the percentage of acinar cells lacking ATRX (n = 3 for all groups). (D) Localization of insulin (green) and ATRX (red) by co-immunofluorescence (IF) demonstrates acinar-specific knockout of ATRX expression in *Mist1^{creERT/+} Atrx^{flΔ18}* mice 20 days after tamoxifen treatment. White arrows indicate ATRX expression in pancreatic duct cells. Sections were counterstained with DAPI to reveal nuclei. Magnification bar = 50 μm.



widespread pancreatic damage.³ Conversely, *MKA* mice demonstrated a variable phenotype based on sex (Figure 8A). Male *MKA* mice ($n = 10$) appeared phenotypically normal with negligible PanIN formation and few pockets of fibrosis relative to *Mist1^{creERT/+}Kras^{LSL-G12D/+}* mice. Conversely, all female *MKA* mice ($n = 6$) developed PanINs and fibrosis, with some mice displaying extensive inflammation and fibrosis, along with disruptions in acinar cell organization consistent with a chronic pancreatitis phenotype (Figure 8A). Trichrome staining confirmed increased fibrosis only in female *MKA* pancreatic tissue relative to *Mist1^{creERT/+}Kras^{LSL-G12D/+}* mice (Figure 9A), and Alcian blue histology confirmed increases in neoplastic PanIN lesions (Figure 9B). The tissue showed significant variability in fibrosis between mice in both *MKA* and *Mist1^{creERT/+}Kras^{LSL-G12D/+}* cohorts (Figure 9C), although female *MKA* mice in general had increased damage (*MKA* = $15.2\% \pm 9.2\%$ damaged area vs *Mist1^{creERT/+}Kras^{LSL-G12D/+}* = $5.0\% \pm 1.6\%$), whereas male *MKA* mice had decreased damage (*MKA* = $0.2\% \pm 0.2\%$ vs *Mist1^{creERT/+}Kras^{LSL-G12D/+}* = $5.8\% \pm 3.8\%$). On the basis of a 2-way ANOVA, no significant differences were observed between any group regarding damaged (ie, lesion) area. However, quantification of lesion type (Figure 9D) indicated significantly more pre-cancerous lesions develop in female *MKA* mice relative to all groups except *Mist1^{creERT/+}Kras^{LSL-G12D/+}* male mice. Quantification of overall pancreatic fibrosis, inflammation, and ADM, as described earlier, confirmed increased injury in *MKA* females relative to *Mist1^{creERT/+}Kras^{LSL-G12D/+}* counterparts (Table 3).

To assess PanIN formation within *Mist1^{creERT/+}Kras^{LSL-G12D/+}* and *MKA* pancreatic tissue, the percentage of pancreatic lobules containing at least one instance of each lesion type (ranging from ADM to PanIN3) was quantified on H&E stained sections (Figure 8B) and statistically compared by 2-way ANOVAs (Table 4). *MKA* female mice had significantly fewer lobules consisting only of normal acini relative to all other groups (Table 4, $P < .05$). Whereas both *Mist1^{creERT/+}Kras^{LSL-G12D/+}* and *MKA* mice exhibited ADM, the incidence of PanIN1 in female *MKA* mice was 2.5-fold higher ($16.21\% \pm 8.3\%$ of lobules; $n = 10$) relative to female *Mist1^{creERT/+}Kras^{LSL-G12D/+}* mice ($6.52\% \pm 3.5\%$; $n = 6$), and female *MKA* mice contained significantly more lobules with PanIN2 lesions than all other genotypes and sexes (Figure 8B, Table 4; $P < .01$). Interestingly, histologic analysis of male *MKA* mice revealed no PanIN1 or PanIN2 lesions (Figure 8B, Table 4).

To determine whether presumptive ADM and PanINs were arising from ATRX null acinar cells, we examined the expression of transcription factors involved in ADM. SOX9 (Figure 10A and B) and PDX1 (data not shown)

accumulation was assessed by immunofluorescence and immunohistochemistry, respectively. As observed earlier, no SOX9+ acinar cells were observed in *Mist1^{creERT/+}* and *Mist1^{creERT/+}Atrx^{flΔ18}* mice. Similarly, *Mist1^{creERT/+}Kras^{LSL-G12D/+}* tissue was devoid of SOX9+ acinar cells, although pockets of putative SOX9+ ADM were observed (Figure 10A). Whereas male *MKA* mice showed few SOX9-expressing cells, SOX9+ cells and ADM were readily apparent in female *MKA* mice (Figure 10A and B). This widespread SOX9 accumulation in both ADM and acinar cells adjacent to areas of damage suggested SOX9 expression precedes ADM, which is in support of previous studies indicating SOX9 expression is required for ADM. Similar increases for PDX1 were observed in female *MKA* tissue, with PDX1+ cells readily observed in ADM and PanINs (data not shown) compared with all other genotypes. In many cases, cells within ADMs and PanIN lesions also stained for Ki67 (Figure 10B), indicating an increase in proliferation in these areas. Quantification of Ki67+ acinar cells showed no significant difference between genotypes, suggesting that proliferation likely occurs after ADM (Figure 10C).

This expression pattern of SOX9 suggests normal progression through ADM in *MKA* mice but does not indicate whether ADM arises from ATRX-positive cells. Therefore, ATRX accumulation was examined to confirm an acinar cell origin for ADM and PanINs. All presumptive ADM observed in male *Mist1^{creERT/+}Kras^{LSL-G12D/+}* mice tissue was ATRX positive. Similarly, all ADM and PanINs in female *Mist1^{creERT/+}Kras^{LSL-G12D/+}* tissue contained exclusively ATRX-positive cells. In *Mist1^{creERT/+}Kras^{LSL-G12D/+}Atrx^{flΔ18/x}* female mice, which harbor one transcriptionally active copy of the *Atrx* gene, ADM and PanINs contained mixed populations of ATRX+ and ATRX- cells. Fifty-nine percent \pm 17% of lesions contained at least 1 ATRX+ cell, with the other 41% \pm 17% lesions containing only ATRX-negative cells (Figure 10D and E). The ATRX- lesions likely arise from cells in which the non-targeted *Atrx* gene has been silenced as part of X chromosome inactivation. Although some ATRX+ cells were observed in PanINs and ADMs of *MKA* mice, the majority of lesions were completely devoid of ATRX expression in male ($82\% \pm 7\%$) and female ($73\% \pm 10\%$) mice. Because ATRX is ubiquitously expressed, the absence of ATRX in PanINs and ADM suggests the origin of these lesions in *MKA* mice as acinar cells.

Finally, to determine whether sex-specific susceptibility conferred by the absence of ATRX on KRAS mice translates to humans, we queried the International Cancer Genome Consortium (dcc.icgc.org) database for ATRX mutations (Figure 11). The International Cancer Genome Consortium database includes whole genome sequence analysis for 729 patients from Australian and Canadian tumor sequencing

Figure 2. (See previous page). Mature acinar cells do not require ATRX for maintenance, but ATRX loss induces low levels of pancreatic damage. (A) Representative H&E staining of *Mist1^{creERT/+}* (WT) and *Mist1^{creERT/+}Atrx^{flΔ18}* (*Atrx^{flΔ18}*) pancreatic tissue 60 days after last tamoxifen gavage. Intralobular adipocytes are indicated by *. (B–D) Representative images and quantification for (B) Ki67 immunofluorescence (*Mist1^{creERT/+}* [WT; $n = 4$]; *Mist1^{creERT/+}Atrx^{flΔ18}* [ATRX-; $n = 5$]), (C) TUNEL (*Mist1^{creERT/+}*, $n = 9$; *Mist1^{creERT/+}Atrx^{flΔ18}*, $n = 10$), or (D) γ H2AX IF (*Mist1^{creERT/+}* [$n = 7$]; *Mist1^{creERT/+}Atrx^{flΔ18}* [$n = 11$]) 60 days after tamoxifen treatment. White arrows indicate positive cells. Magnification bar = 50 μ m. Data were assessed by using two-tailed *t* test with Tukey post hoc test. Error bars represent means \pm standard error; * $P < .005$.

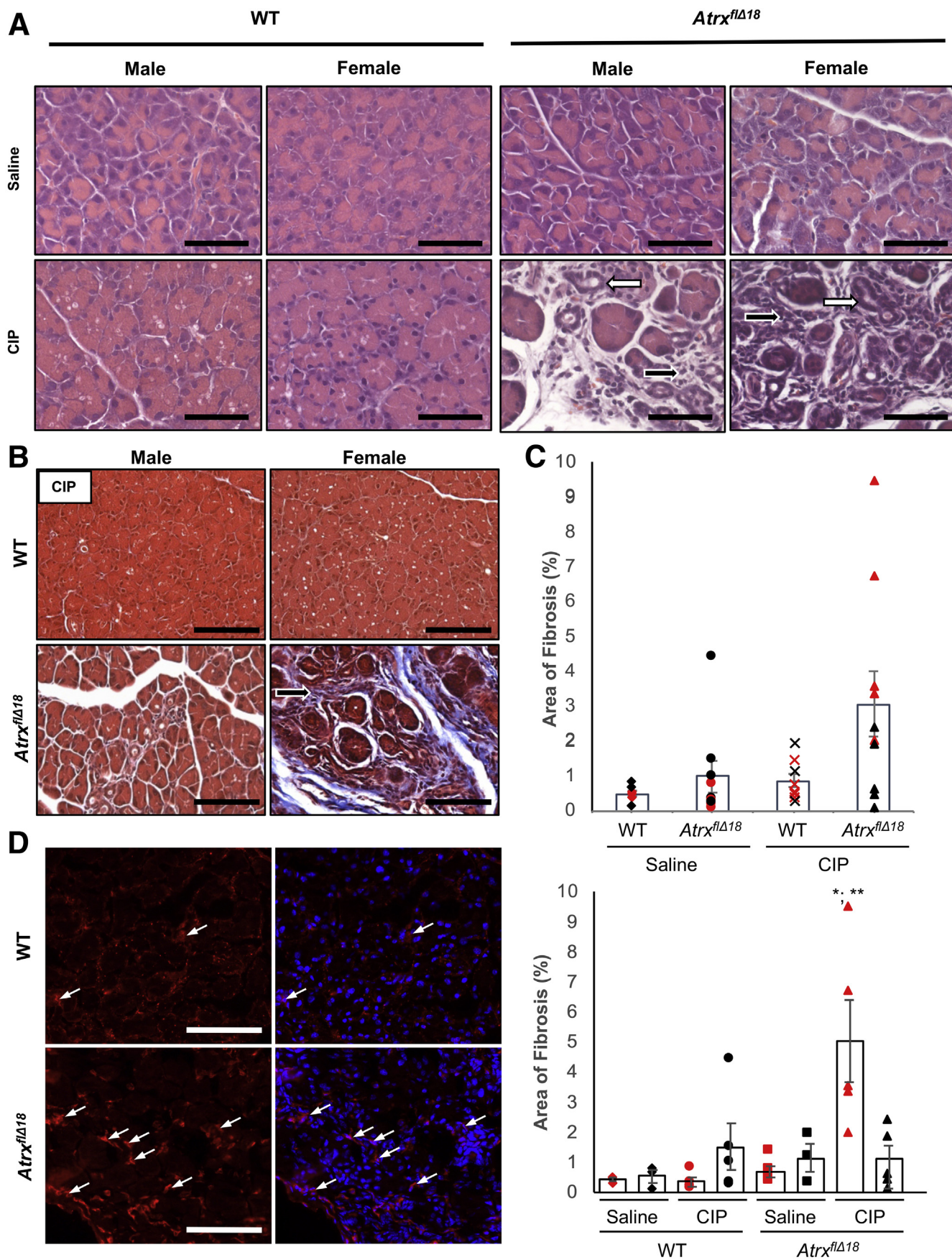


Table 1. Histology Grading Criteria

ADM (based on worst pancreatic lobule)		Fibrosis (based on trichrome stain)	
0	None present	0	None present
1	>10% of lobule	1	<5% of tissue area
2	10%–30% of lobule	2	5%–10% of tissue area
3	30%–50% of lobule	3	10%–20% of tissue area
4	>50% of lobule	4	>20% of tissue area
Inflammation			
0	None present		
1	Focal: small, contained areas		
2	Mild: small, slightly diffuse areas		
3	Moderate: diffuse areas		
4	Severe: diffuse areas, significant presence throughout the tissue		

NOTE. Grading of pancreatic lesions: pancreatic lesions (ranging from ADM to PanIN grade 3) were quantified and classified into the following categories: ADM, PanIN grade 1, PanIN grade 2, PanIN grade 3, or PDAC based on morphologic characteristics including cell shape (cuboidal or columnar), presence of mucin accumulation, nuclear atypia, pseudostratification, and papillary or cribriform structure.

studies and consists of 324 female patients (42%) and 405 male patients (53%). Gender was not identified in 5% of the patients. Therefore, the proportion of PDAC patients reported as female was 0.44. *KRAS* mutations were identified in 591 patients, with a similar ratio of male (55%) to female (45%) patients. Two hundred sixty-eight mutations were observed within the *ATRX* gene, encompassing 145 (~19%) PDAC patients, with 68% of *ATRX* mutations in female patients. Therefore, the proportion of PDAC patients carrying *ATRX* mutations that were female was 0.68. The difference in proportions is significant, $\chi^2(1, N = 729) = 41.633$; $P < .00001$ (Figure 11B), suggesting *ATRX* mutations are related to the sex of the patient.

Most *ATRX* mutations in both sexes are found in non-coding regions, and the impact on expression is unknown. However, 8 patients harbor *ATRX* mutations with a predicted impact on protein function. All but one of these mutations occur in female patients, suggesting a sex-specific

susceptibility in the human patient population. Pancreatic neuroendocrine and glioblastoma patient populations show 46% and 42% of the identified *ATRX* mutations are in female populations. Conversely, 60% of the *ATRX* mutations found in the pediatric brain tumor population occur in female patients. However, χ^2 analysis indicates the proportions of *ATRX* mutations are independent of sex (Figure 11C and data not shown). Interestingly, mutations in *DAXX*, the partner for *ATRX* in depositing H3.3 variant histones into chromatin,^{11,12} are rare in PDAC and show no sex bias. Other common mutations linked to PDAC, including *P16/CDNK2* (Figure 11A) and *SMAD4* (data not shown), showed no sex bias.

Discussion

Pancreatic ductal adenocarcinoma is currently the third leading cause of cancer-related deaths in North America (www.pancan.org). Five-year survival rates have increased only marginally in the last 30 years because of late stage of diagnosis and insensitivity to conventional chemotherapeutics. Therefore, detecting factors that increase sensitivity of pancreatic tissue to the oncogenic properties of mutated *KRAS* is important in identifying alternative therapeutic and diagnostic options. In this study, we have shown that acinar-specific loss of *ATRX*, a chromatin remodelling protein, affects the tissue's response to injury and constitutive mutant *KRAS* activity. Using a novel mouse line that allows for acinar-specific ablation of *Atrx*, we show loss of *ATRX* increased the sensitivity for pancreatic injury. In addition, we showed loss of *Atrx* dramatically enhanced the ability of oncogenic *KRAS* to promote precancerous lesions in the pancreas. Importantly, these effects were observed in a sex-specific fashion, with only female mice displaying sensitivity to loss of *ATRX*. Our results also suggest that loss of *ATRX* may reduce the sensitivity to oncogenic *KRAS* in male mice. This is evidence of a sex-specific susceptibility factor and suggests stratification of PDAC based on their molecular profile may identify new targets for therapy and diagnosis.

Although we have not defined a role for *ATRX* in normal acinar cell physiology, it appears *ATRX* is dispensable for maintaining the acinar cell phenotype in the adult. This is consistent with previous studies that identified roles for *ATRX* only in mitotically active tissue, where loss of *ATRX*

Figure 3. (See previous page). **Loss of *ATRX* sensitizes acinar tissue to recurrent pancreatic injury 3 days after cessation of pancreatic injury.** (A) H&E staining of saline or cerulein (CIP) treated *Mist1^{creERT/+}* (WT) and *Mist1^{creERT/+} Atrx^{flΔ18}* (*Atrx^{flΔ18}*) mice. CIP-treated *Mist1^{creERT/+}* mice show vacuolation and intra-acinar edema relative to saline-treated mice. CIP-treated *Mist1^{creERT/+} Atrx^{flΔ18}* mice demonstrated increased damage (black arrows) and putative ADM (white arrows) relative to CIP-treated *Mist1^{creERT/+}* mice. Magnification bar = 50 μ m. (B) Trichrome stain of *Mist1^{creERT/+}* and *Mist1^{creERT/+} Atrx^{flΔ18}* tissue indicating fibrosis. *Mist1^{creERT/+} Atrx^{flΔ18}* mice exhibit increased fibrosis (black arrow) and to a greater extent in female *Mist1^{creERT/+} Atrx^{flΔ18}* mice. Magnification bar = 100 μ m. (C) Quantification of fibrosis in pancreatic tissue from *Mist1^{creERT/+}* (WT) mice treated with saline (n = 4 female or 3 male) or cerulein (n = 4 female or 5 male) and *Mist1^{creERT/+} Atrx^{flΔ18}* (*Atrx^{flΔ18}*) mice treated with saline (n = 5 female or 3 male) or cerulein (n = 5 female and male). Male mice are denoted as black symbols and female mice as red symbols. Data were assessed using 2-way ANOVA with Tukey post hoc test. Error bars represent means \pm standard error. When not considering sex (upper graph), no significant differences exist between groups. When sex of the mouse is considered (lower graph), female CIP-treated *Mist1^{creERT/+} Atrx^{flΔ18}* mice are significantly different than all groups (* $P < .05$ vs all male mouse groups; ** $P < .01$ vs female *Mist1^{creERT/+}* and *Mist1^{creERT/+} Atrx^{flΔ18}* saline-treated and female *Mist1^{creERT/+}* CIP-treated groups). Individual animals are denoted with black (male) or red (female) markers. (D) Representative immunofluorescent images of F4/80 accumulation in CIP-treated female *Mist1^{creERT/+}* and *Mist1^{creERT/+} Atrx^{flΔ18}* tissue (repeated 3 times). Arrows indicate macrophages. Sections were counterstained with DAPI. Magnification bar = 70 μ m.

Table 2. Morphometric Analysis of Pancreatic Tissue After Recurrent Pancreatic Damage

	Male		Female	
	<i>Mist1</i> ^{creERT/+} (5)	<i>Mist1</i> ^{creERT/+} <i>Atrx</i> ^{flΔ18} (5)	<i>Mist1</i> ^{creERT/+} (4)	<i>Mist1</i> ^{creERT/+} <i>Atrx</i> ^{flΔ18} (5)
Fibrosis	0 ± 0	0 ± 0	0 ± 0	1.4 ± 0.51
Inflammation	0.2 ± 0.20	1.4 ± 0.25	0.75 ± 0.25	2.4 ± 0.40
ADM	0 ± 0	0.6 ± 0.25	0 ± 0	1.2 ± 0.37
Total	0.2 ± 0.2	2.0 ± 0.45	0.75 ± 0.25	5.0 ± 1.1 ^a

NOTE. (#) indicates n value; see methodology for scoring. Histopathologic assessment of pancreatic damage, as indicated by 3 factors: fibrosis, inflammation, and presence of ADM. Scores are represented on a grading scale from 0 to 4. Superscript letter “a” indicates groups that are statistically different ($P < .01$). Data were assessed using 2-way ANOVA and Tukey post hoc test.

maintains genomic stability and regulates cell cycle processes including proper chromosome segregation during mitosis.^{14,27} We did observe small, yet significant increases in acinar cell apoptosis, dsDNA damage, and proliferation in *Mist1*^{creERT/+}*Atrx*^{flΔ18} mice, suggesting during a longer period of time (>2 months), the absence of ATRX may lead to more overt damage. Acinar cell division in the adult rodent pancreas is <2%,³⁰ which is similar to the observed rates of apoptosis and dsDNA damage. However, targeted ablation of other factors, including *Xbp1*³¹ and *Pdx1*,³² results in rapid loss of acinar tissue, so acinar cell division is clearly not a prerequisite for development of overt pancreatic pathologies. Mild damage in acinar tissue with ATRX loss suggested acinar cells may be sensitive to other factors known to promote pancreatic pathologies.

When exposed to recurrent cerulein treatment, only *Mist1*^{creERT/+}*Atrx*^{flΔ18} mice showed fibrosis, inflammatory cell infiltration, and regions of ADM, with the effects more dramatic in female mice. It is unclear whether loss of ATRX leads to increased damage or if regeneration is impaired in *Mist1*^{creERT/+}*Atrx*^{flΔ18} mice. Unpublished work from our laboratory using an acute pancreatitis regimen indicated similar amounts of damage in control and *Mist1*^{creERT/+}*Atrx*^{flΔ18} mice immediately after injury, suggesting loss of ATRX impairs the regenerative process after injury, and is consistent with studies in which other chromatin remodeling proteins (EZH2³³ and BMI1¹⁰) are required for proper pancreatic regeneration. It is possible that defects from *Atrx* loss become more widespread once injury is induced, and increased DNA damage and/or replicative defects provide a barrier to acinar tissue regeneration. However, we found no differences in apoptosis and proliferation in cerulein-treated mice, suggesting these are not contributing factors through which ATRX loss promotes damage.

The combination of *Atrx* deletion with oncogenic KRAS activation produced extensive fibrosis and inflammation, pancreatic damage indicative of chronic pancreatitis, as well as PanIN lesions up to grade 2. In this instance, damage was exclusive to female mice. Consistent with previous studies,³⁴ we observed minimal fibrosis and PanIN lesions in KRAS mice that indicate oncogenic KRAS activation in adult mice required another stimulus, such as chronic pancreatitis, to produce invasive PDAC. The pancreatic injury observed in

the female *MKA* mice suggests that chronic pancreatitis occurs in these mice, and the inflammation observed may contribute to increased susceptibility to active KRAS. Loss of function mutations in ATRX have been identified in other cancer types, most notably those involving up-regulation of the alternative lengthening of telomeres pathway.^{13,35} Mutations in ATRX or binding partner DAXX are often observed in pancreatic neuroendocrine tumors and glioblastomas, but neither cancer shows a gender preference with or without ATRX mutation. Studies examining PDAC tumors confirmed an absence of alternative lengthening of telomeres in every case,³⁶ and PDAC is typically characterized by telomere attrition.³⁷ Therefore, we suggest that ATRX is affecting an alternative pathway in PDAC, possibly in a DAXX-independent manner. ATRX interacts with enhancer of zeste homologue 2 (EZH2), a member of polycomb repressor complex 2, leading to altered gene expression,³⁸ and loss of EZH2 also increases sensitivity to oncogenic KRAS.³³

The incidence of human PDAC between sexes is relatively equal, with approximately the same number of cases occurring in men and women (Canadian Cancer Statistics, 2016). Assessment of International Cancer Genomic Consortium database revealed ATRX single nucleotide polymorphisms in almost 20% of PDAC cases (145/729), although most were in non-coding regions of the gene. However, whether in the coding or non-coding regions, ATRX mutations had a higher than expected frequency in female patients, even when taking into consideration that it is an X-linked gene. Therefore, it is possible that ATRX loss defines a unique subtype of PDAC, in which female patients are more susceptible, or that loss of ATRX function in male patients does not allow progression through to a PDAC phenotype. Although we have observed decreased acinar cell sensitivity to oncogenic KRAS in male mice, female *MKA* mice show significantly increased progression to PanIN1 and PanIN2 lesions, and the mechanisms underlying the extensive pancreatic damage specifically in female *MKA* mice are unclear. It is possible that loss of ATRX enhances KRAS activity and leads to altered hormonal signalling. Sex hormone receptors, including estrogen receptors, play a role in the progression of other cancers such as colorectal cancer.³⁹ However, the *Atrx* gene is located on the X

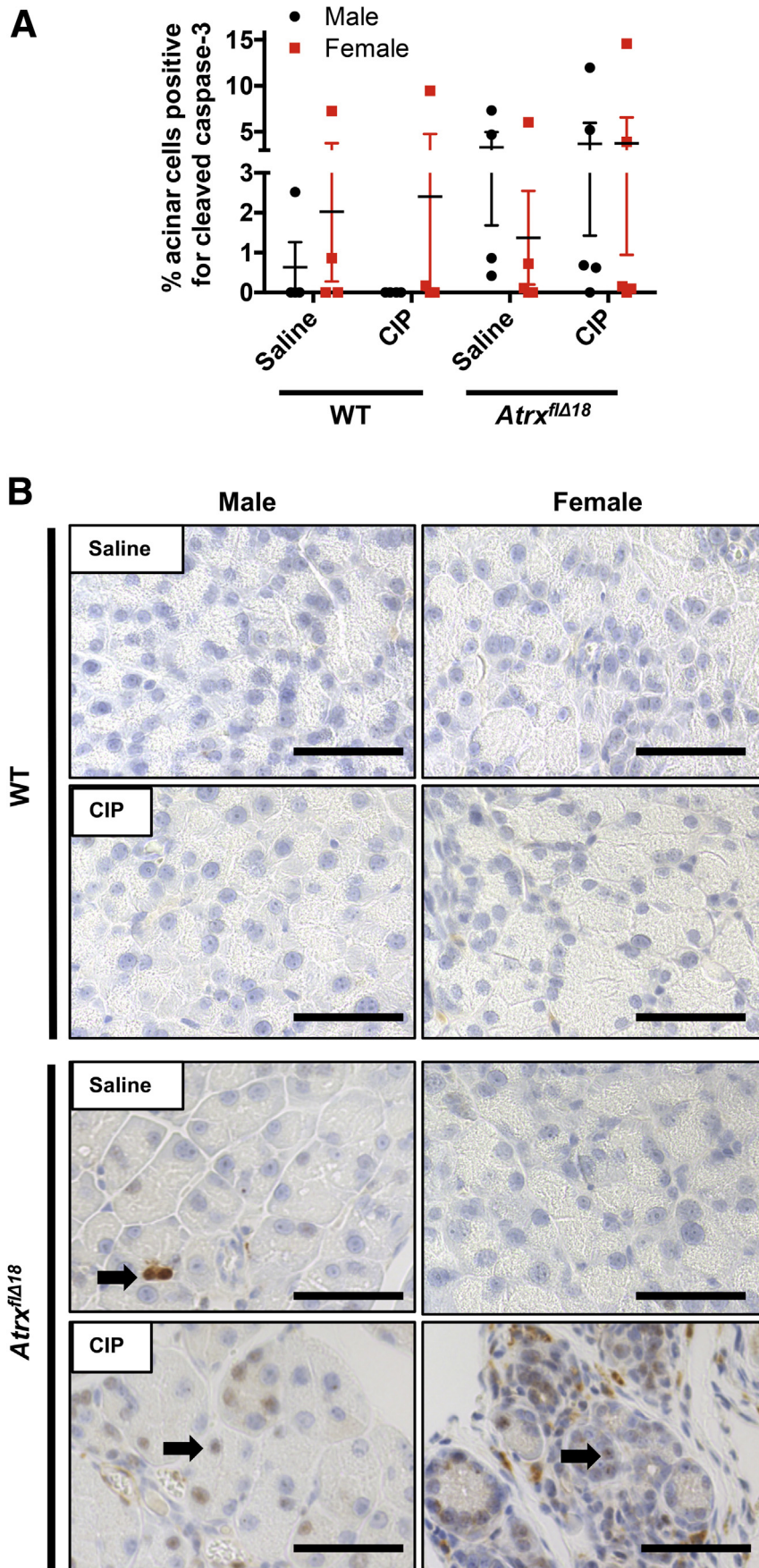
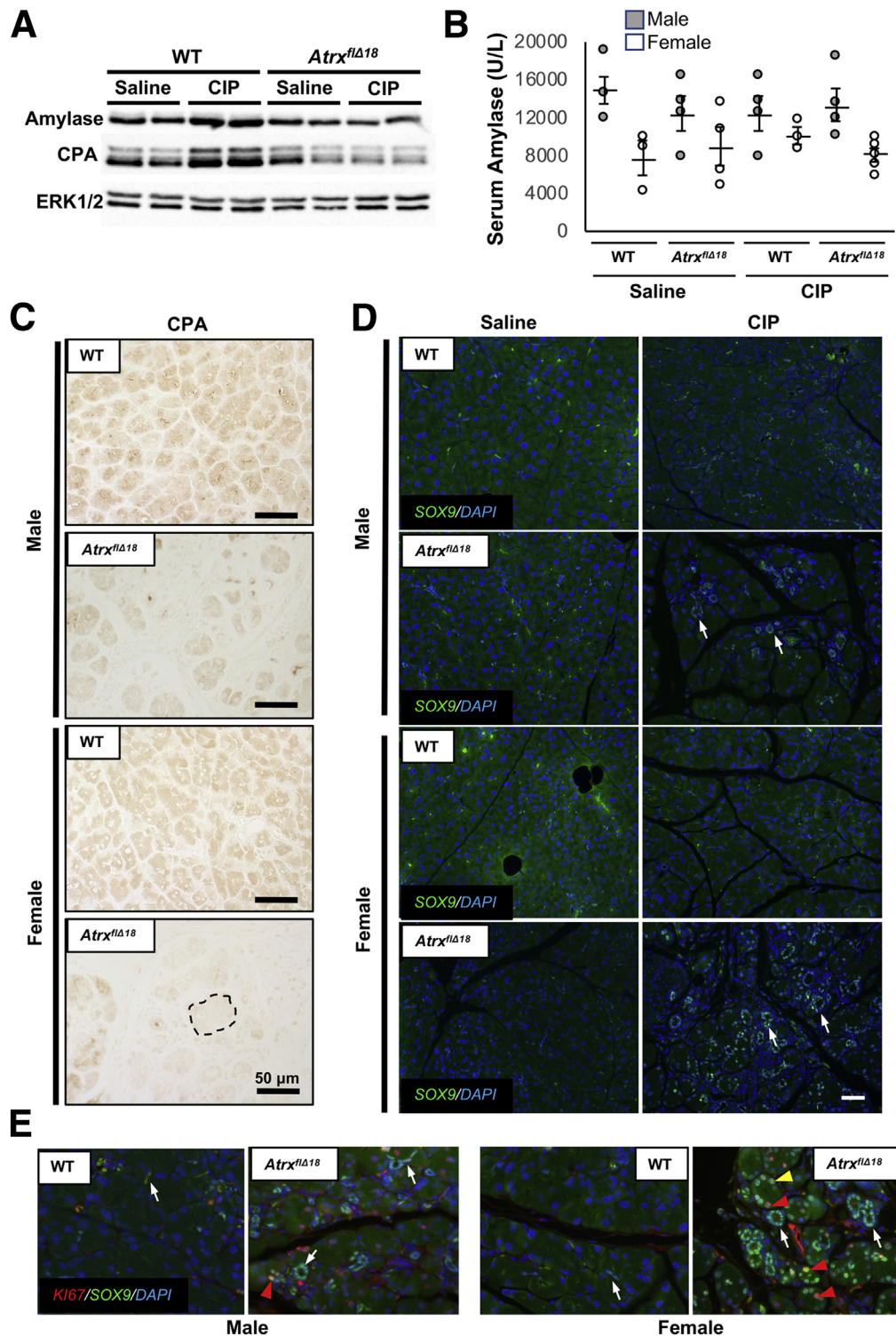


Figure 4. *Mist1^{creERT/+} Atrx^{flΔ18}* pancreatic tissue shows increased apoptosis after recurrent CIP treatment. (A) Acinar cell-specific cleaved caspase-3 comparing *Mist1^{creERT/+}* (WT) and *Mist1^{creERT/+} Atrx^{flΔ18}* (*Atrx^{flΔ18}*) pancreatic tissue after saline (SAL) or cerulein (CIP) treatment. Quantification in pancreatic tissue from *Mist1^{creERT/+}* (WT) mice treated with saline (n = 4 female or 3 male) or cerulein (n = 4 female or 5 male) and *Mist1^{creERT/+} Atrx^{flΔ18}* (*Atrx^{flΔ18}*) mice treated with saline (n = 5 female or 4 male) or cerulein (n = 5 female and male). Data were assessed using 2-way ANOVA with Tukey post hoc test. Error bars represent means \pm standard error. (B) Immunohistochemistry for cleaved caspase-3 in male and female *Mist1^{creERT/+}* (WT) or *Mist1^{creERT/+} Atrx^{flΔ18}* pancreatic tissue 3 days after cessation of cerulein treatment. Arrows indicate apoptotic cells. Magnification bar = 50 μ m.

Figure 5. *Mist1*^{creERT/+} + *Atrx*^{flΔ18} pancreatic tissue shows reduced regeneration after recurrent CIP treatment. Tissue was examined 3 days after cessation of recurrent CIP treatment. (A) Western blot analysis for CPA, amylase, SOX9, and total ERK1/2 (tERK1/2; loading control). Increased accumulation of digestive enzymes was observed specifically in *Mist1*^{creERT/+} (WT) mice, whereas *Mist1*^{creERT/+} + *Atrx*^{flΔ18} (*Atrx*^{flΔ18}) mice did not demonstrate similar accumulation. (B) Serum amylase levels in mice (n = 3–4 for each group). Data were assessed by using 2-way ANOVA with Tukey post hoc test. Bars represent mean ± standard error. No significant difference in body weight or amylase levels was observed between genotypes. (C) Immunohistochemistry for CPA in *Mist1*^{creERT/+} or *Mist1*^{creERT/+} + *Atrx*^{flΔ18} mice. CPA accumulation was decreased in female *Mist1*^{creERT/+} + *Atrx*^{flΔ18} mice (acinus is indicated by dotted line). (D) Representative immunofluorescence for SOX9 (green) expression was increased in male *Mist1*^{creERT/+} + *Atrx*^{flΔ18} and female *Mist1*^{creERT/+} + *Atrx*^{flΔ18} tissue (white arrows). Magnification bars = 50 μm. (E) Higher magnification images show SOX9 expression in duct, putative ADM (white arrows), and acinar cell (yellow arrowheads). Sections were co-stained for Ki-67 (red arrowheads) and counterstained with DAPI.



chromosome and is a target of X inactivation. Therefore, it would be expected that female mice heterozygous (*Atrx*^{flΔ18/x}) for the mutant *Atrx* allele would also show similar effects because approximately half of the acinar cells lose ATRX expression. Immunohistochemistry for ATRX confirmed that at least a portion of acinar cells in heterozygous *Atrx*^{flΔ18/x}

mice did lose ATRX expression (data not shown), but these mice did not demonstrate increased damage or susceptibility to oncogenic KRAS. These results suggest complete loss of ATRX is required for enhanced KRAS activity and pancreatic damage to occur in female mice. However, such a model also does not account for decreased sensitivity in male MKA mice.

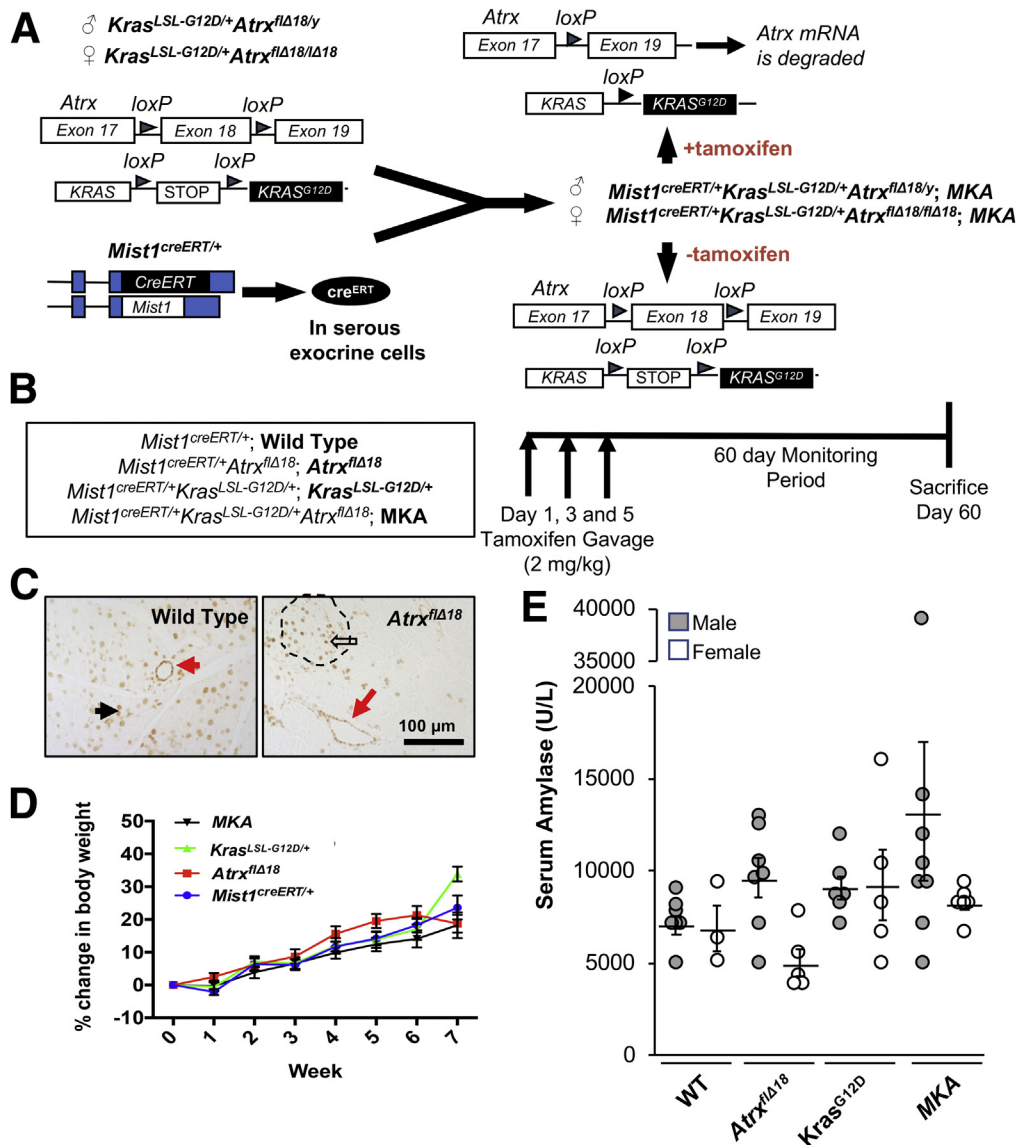


Figure 6. Induction of oncogenic KRAS with *Atrx* deletion. (A) Schematic of *Atrx*-deficient mouse model with oncogenic KRAS activation. (B) Experimental timeline for tamoxifen gavage in congenic *Mist1*^{creERT/+}, *Mist1*^{creERT/+}*Atrx*^{flΔ18}, *Mist1*^{creERT/+}*Kras*^{LSL-G12D/+}, and MKA mice. Names used for each line within the figures are depicted in bold. (C) Immunohistochemistry for ATRX in acinar (black arrow) and duct (red arrow) cells of *Mist1*^{creERT/+} and *Mist1*^{creERT/+}*Atrx*^{flΔ18} mice, ATRX expression is limited to islet (open arrow; delineated by dotted line) and duct cells (red arrow). (D) Change in body weight (%) of mice after *Atrx* deletion ± oncogenic KRAS activation. Mouse genotypes include *Mist1*^{creERT/+} (WT; n = 13), *Mist1*^{creERT/+}*Atrx*^{flΔ18} (*Atrx*^{flΔ18}; n = 12), *Mist1*^{creERT/+}*Kras*^{LSL-G12D/+} (*Kras*^{LSL-G12D/+}; n = 17), and MKA (n = 16). Points are represented as mean weight ± standard error. (E) Serum amylase levels in WT (n = 7 male or 3 female), *Atrx*^{flΔ18} (n = 7 male or 5 female), *Kras*^{LSL-G12D/+} (n = 6 male or 5 female), and MKA (n = 8 male or 6 female) mice 60 days after *Atrx* deletion ± oncogenic KRAS activation. Data were assessed using 2-way ANOVA with Tukey post hoc test. Bars represent mean ± standard error.

Sex-specific mechanisms could also be explained by a difference in inflammatory response. It is possible that female *Atrx*^{flΔ18/flΔ18} mice are more susceptible to factors promoting inflammation. During recurrent pancreatic injury, *Atrx*^{flΔ18/flΔ18} mice showed increased inflammation in comparison with male counterparts, resulting in higher levels of damage. In combination with oncogenic KRAS, increased inflammation in *Atrx*^{flΔ18/flΔ18} mice may amplify KRAS activity and activation of downstream pathways, including MAPK and PI3K-PDK1-Akt signaling, leading to

increased cell survival and proliferation. Accordingly, increased *KRAS*^{G12D} activity by inflammatory cytokines (nuclear factor kappa B, interleukin 6) has been demonstrated previously.^{40,41} The presence of an inflammatory response in female *Atrx*^{flΔ18/flΔ18} mice, which is not observed in male *Atrx*^{flΔ18/y} mice, could lead to increased damage.

It is also possible that sex-specific differences exist regarding the function of SOX9. Previous work suggests SOX9 is required for initiation of ADM,⁴ and we show



Figure 7. Gross morphology does not reveal significant differences on dissection. *Mist1*^{creERT/+} (WT), *Mist1*^{creERT/+} *Atrx*^{flΔ18} (*Atrx*^{flΔ18}), *Mist1*^{creERT/+} *Kras*^{LSL-G12D/+} (*Kras*^{LSL-G12D/+}), or MKA mice. Although female MKA mice may show some edema, the only easily identified difference is splenomegaly (*), which consistently appeared in *Mist1*^{creERT/+} *Kras*^{LSL-G12D/+} and MKA mice.

increased SOX9 accumulation in female MKA acinar cells surrounding damage. Increased susceptibility in female MKA mice could include sex-specific hormonal or inflammatory pathways that provoke increased SOX9 expression. As mentioned, female *Atrx*^{flΔ18/flΔ18} mice have an amplified inflammatory response, and inflammatory signaling pathways can influence SOX9 expression during development.⁴² Alternatively, hormonal factors could play a role in sex-specific *Sox9* regulation. Recently, up-regulation of estrogen receptor α -receptor activity in breast cancer cells has been associated with increased SOX9 expression, although this study occurs in the context of estrogen deprivation.⁴³

It would be interesting to observe the long-term effects of ATRX deletion on oncogenic KRAS-mediated PDAC formation. Because of the prevalence of tumors developing in the oral mucosa, we were forced to kill MKA mice before overt PDAC development. These tumors likely arise because of the expression of *Mist1*^{creERT} in other tissues, and we are currently generating *Atrx*^{flΔ18/flΔ18} mice with a pancreas-specific inducible cre-recombinase, which will allow for longer-term analysis. It is possible that having only a single copy of *Mist1* contributes to the *Mist1*^{creERT/+} *Atrx*^{flΔ18} and MKA phenotypes. Although previous studies⁴⁴ and unpublished work from our laboratory demonstrated no difference in the phenotype between mice heterozygous or wild-type (WT) for *MIST1* expression, using a different cre-recombinase (such as *Ptf1a*^{creERT}) would rule out any contribution of *Mist1* haploinsufficiency to the results observed in this study.

In summary, we identified that loss of ATRX enhanced pancreatic injury and susceptibility to KRAS-mediated pancreatic damage. Potential gender-specific factors within *Atrx*^{flΔ18/flΔ18} mice (including hormonal factors or increased

inflammation) provide an additional driving factor for KRAS activity and pancreatic damage, leading to a female-specific phenotype.

Materials and Methods

Animal Generation and Cre Induction

Mouse experiments were approved by the Animal Care and Use Committee at Western University (Protocol #2017-001). All mice used in this study were maintained in a C57Bl6 background. Mice expressing *creERT* from the *Mist1* locus (*Mist1*^{creERT/+})⁵ were crossed with mice harboring an *Atrx* allele with exon 18 flanked by loxP sites,²³ producing male (*Mist1*^{creERT/+} *Atrx*^{flΔ18/y}) and female (*Mist1*^{creERT/+} *Atrx*^{flΔ18/flΔ18}) mice, collectively referred to as *Mist1*^{creERT/+} *Atrx*^{flΔ18}. *Mist1*^{creERT/+} *Atrx*^{flΔ18} mice were crossed to mice containing an inducible oncogenic *KRAS* (*loxP-STOP-loxP* (*LSL*)-*KRAS*^{G12D})⁴⁵ to produce *Mist1*^{creERT/+} *Kras*^{LSL-G12D/+} *Atrx*^{flΔ18} mice (referred to as MKA). Furthermore, female mice containing one (*Mist1*^{creERT/+} *Atrx*^{flΔ18/x}) or two (*Mist1*^{creERT/+} *Atrx*^{x/x}) copies of the *Atrx* allele showed no obvious phenotypic differences and were combined as a single *Mist1*^{creERT/+} control group. Female mice expressing *KRAS*^{G12D} that were heterozygous (*Mist1*^{creERT/+} *Kras*^{LSL-G12D/+} *Atrx*^{flΔ18/x}) or homozygous for *Atrx* (*Mist1*^{creERT/+} *Kras*^{LSL-G12D/+} *Atrx*^{x/x}) also showed no obvious morphologic differences and were collectively referred to as *Mist1*^{creERT/+} *Kras*^{LSL-G12D/+} mice.

Tamoxifen (Sigma-Aldrich, St Louis, MO; cat. #T5648) was administered through oral gavage (2 mg/mouse) 3 times over 5 days. This resulted in >95% recombination in acinar cells and no recombination in duct cells.²⁴ Mice were monitored for 60 days from first tamoxifen gavage, and body weight was measured weekly.

Cerulein Induced Pancreatitis

To induce recurrent pancreatic injury, control (*Mist1^{creERT/+}*) and *Mist1^{creERT/+}Atrx^{flΔ18}* mice were given intraperitoneal injections of saline or cerulein (75 μg/kg body weight; Sigma-Aldrich; cat. #C9026) twice daily for 11 days, followed by a 3-day recovery period. Mice were weighed daily throughout the injury protocol. Mice

were killed and processed for histologic, molecular, biochemical, and blood serum analysis.⁴⁶ Serum amylase was quantified by using Phadebas tablets (Magle Life Sciences, Lund, Sweden; cat. #1302) following manufacturer's instructions.

Histology, Immunohistochemistry, and Immunofluorescent Analysis

The head of the pancreas was used for paraffin sections, and cryostat sections were obtained from the middle portion of pancreas. Tissue was washed 2 times in phosphate-buffered saline and then dehydrated through a series of alcohol washes for embedding into paraffin. Paraffin sections (5 μm) were stained by using standard H&E, Alcian blue (Mucin Stain; Abcam Inc, Cambridge, MA; cat. #ab150662) or Masson's trichrome stain (Abcam Inc; cat. #ab150686) protocols. Sections were imaged by using the Aperio CS2 Digital Scanner and Aperio ImageScope software (Leica Biosystems Imaging Inc, San Diego, CA). Total tissue area was quantified by using the Fiji software,⁴⁷ and area of damage was quantified as a percentage of total area. Levels of pancreatic damage were assessed by using a grading scale based on 3 factors: fibrosis, inflammation, and presence of acinar to ductal metaplasia. Tissue sections were scored by multiple individuals blinded to mouse genotypes on a scale from 0 to 4. Descriptions of each score can be found in Table 1 along with a description of scoring PanIN lesions.

For immunohistochemical analysis, paraffin tissue sections were stained by using the ABC staining system (Santa Cruz Biotechnology Inc, Dallas, TX) or the VectaStain ABC HRP kit with ImmPACT DAB Peroxidase (HRP) Substrate (Vector Laboratories, Brockville, ON, Canada; cat. #SK-4105) according to kit instructions. Cleaved caspase-3 (rabbit 1:100; Cell Signaling Technology, Danvers, MA; cat. #966455) staining was completed by using the Ventana Discovery Ultra XT autostainer (Ventana Medical Systems Inc, Tucson, AZ). Primary antibodies used are specific to ATRX (rabbit; diluted 1:100 in 1.5% mouse blocking serum in phosphate-buffered saline; Santa Cruz Biotechnology Inc; cat. #sc15408), PDX1 (rabbit; 1:1000; Abcam Inc; cat. #ab47267), Ki67 (rabbit 1:500; Abcam Inc; cat. #ab15580). For immunofluorescence, cryostat sections were processed

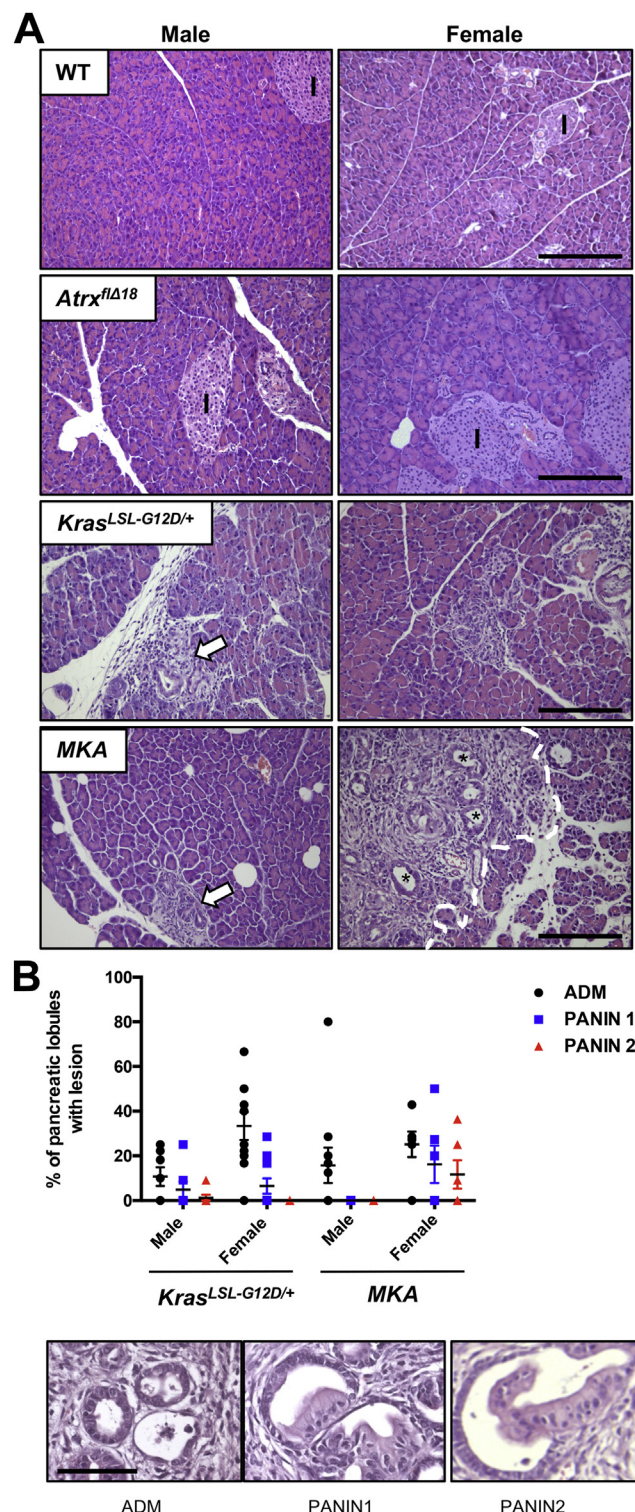


Figure 8. Loss of ATRX enhances *KRAS^{G12D}*'s ability to promote pre-cancerous lesions in female mice. (A) H&E images of pancreatic tissue from male and female *Mist1^{creERT/+}* (WT), *Mist1^{creERT/+}Atrx^{flΔ18}* (*Atrx^{flΔ18}*), *Mist1^{creERT/+}Kras^{LSL-G12D/+}* (*Kras^{LSL-G12D/+}*), and MKA mice 60 days after tamoxifen treatment. Arrows indicate focal ADM or PanIN lesions. Dotted white line delineates significant lesion area from acinar tissue. Islets are indicated by I. Magnification bar = 200 μm. (B) Average percentage of lobules containing at least one instance of ADM, PanIN1, or PanIN2 in *Kras^{LSL-G12D/+}* (n = 7 male or 10 female) and MKA (n = 10 male or 6 female) mice. Data were assessed by using 2-way ANOVA with Tukey post hoc test. Representative examples of ADM, PanIN1, and PanIN2 lesions from female MKA mice. Magnification bars = 50 μm.

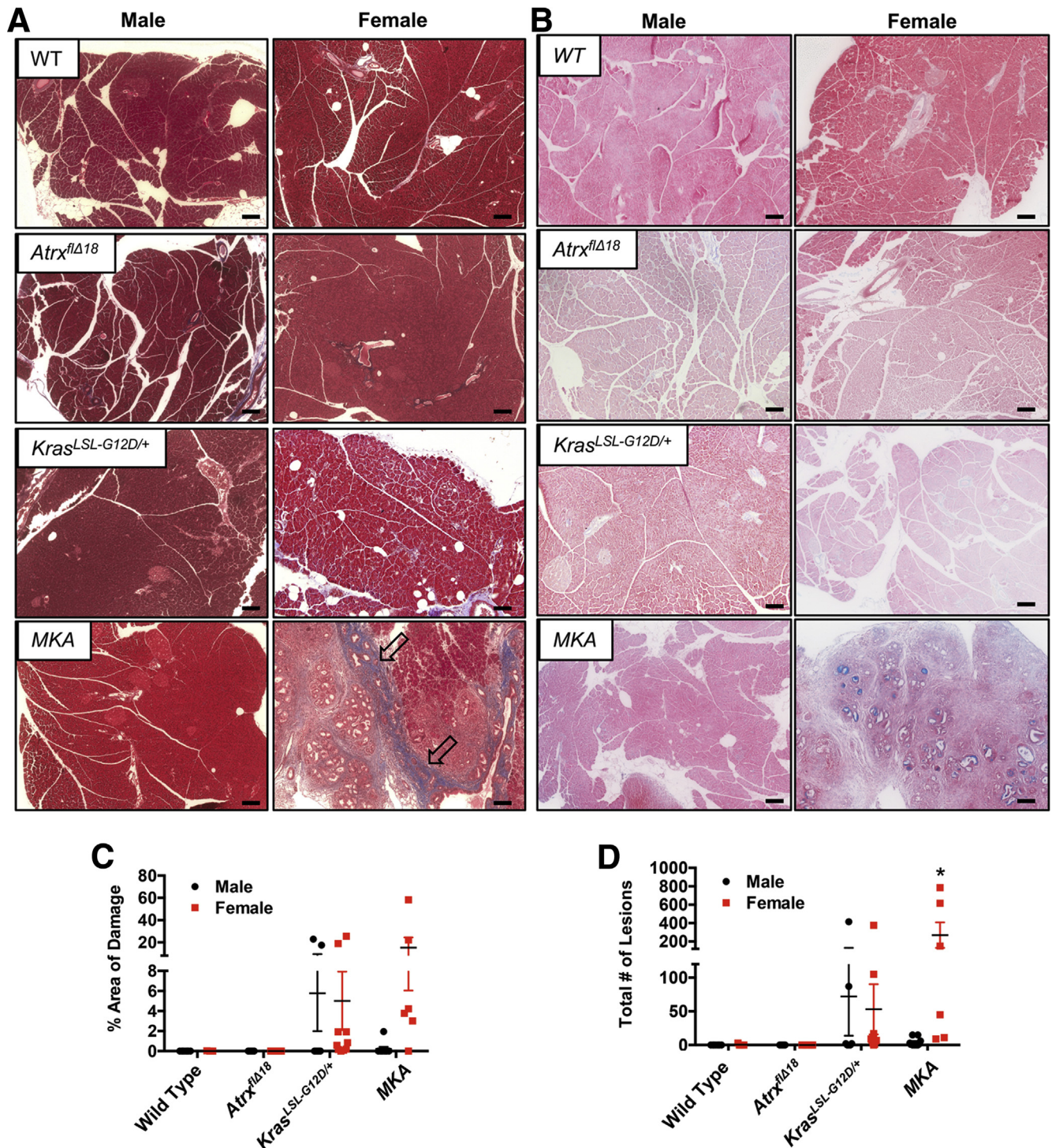


Figure 9. Histology of pancreatic tissue after *Atrx* deletion. Representative (A) trichrome or (B) Alcian blue images of pancreatic tissue from male and female *Mist1^{creERT/+}* (WT), *Mist1^{creERT/+}Atrx^{flΔ18}* (*Atrx^{flΔ18}*), *Mist1^{creERT/+}Kras^{LSL-G12D/+}* (*Kras^{LSL-G12D/+}*), and MKA mice 60 days after tamoxifen treatment. Increased tissue fibrosis was routinely observed in MKA females (arrows). Magnification bar = 200 μ m. Increased fibrosis (open arrow) and duct metaplasia are observed in female MKA tissue. Quantification of (C) damaged area as percentage of total pancreatic area based on appearance of PanINs or fibrosis, or (D) number of ADM and PanINs (lesions) observed within *Mist1^{creERT/+}* (WT; n = 8 male or 5 female), *Mist1^{creERT/+}Atrx^{flΔ18}* (*Atrx^{flΔ18}*; n = 8 male or 5 female), *Mist1^{creERT/+}Kras^{LSL-G12D/+}* (*Kras^{LSL-G12D/+}*; n = 7 male or 10 female), and MKA (n = 10 male or 6 female) mice 60 days after tamoxifen treatment. Number of ADM and PanINs (lesions) was significantly increased in MKA females compared with all other groups except male *Mist1^{creERT/+}Kras^{LSL-G12D/+}* (*Kras^{LSL-G12D/+}*) mice. Data were assessed by using 2-way ANOVA with Tukey post hoc test. Bars represent mean \pm standard error; **P* < .05.

Table 3. Morphometric Analysis of Pancreatic Tissue 60 Days After Activation of KRAS^{G12D} and Loss of *Atrx*

	<i>Mist1</i> ^{creERT/+}		<i>Mist1</i> ^{creERT/+} <i>Atrx</i> ^{flΔ18}		<i>Mist1</i> ^{creERT/+} <i>Kras</i> ^{LSL-G12D/+}		MKA	
	Male (8)	Female (5)	Male (8)	Female (5)	Male (7)	Female (10)	Male (10)	Female (6)
Fibrosis	0 ± 0	0 ± 0	0 ± 0	0 ± 0	1 ± 0.66	0.7 ± 0.47	0 ± 0	1.83 ± 0.48
Inflammation	0 ± 0	0 ± 0	0.14 ± 0.14	0.33 ± 0.21	1 ± 0.54	1 ± 0.52	0.2 ± 0.13	2.17 ± 0.70
ADM	0 ± 0	0.2 ± 0.2	0 ± 0	0 ± 0	1.57 ± 0.65	1.5 ± 0.45	0.4 ± 0.16	3 ± 0.45
Total	0 ± 0 ^a	0.2 ± 0.2 ^a	0.14 ± 0.14 ^a	0.33 ± 0.21 ^a	3.57 ± 1.8 ^{a,b}	3.2 ± 1.4 ^{a,b}	0.6 ± 0.27 ^a	7 ± 1.57 ^b

NOTE. (#) indicates n value; see methodology for scoring. Histopathologic assessment of pancreatic damage, as indicated by 3 factors: fibrosis, inflammation, and presence of ADM. Scores are represented on a grading scale from 0 to 4. Superscript letters "a" and "b" indicate groups that are statistically different ($P < .01$). Data were assessed using 2-way ANOVA and Tukey post hoc test.

as previously described.⁴⁶ Primary antibodies used were specific to ATRX (rabbit; diluted 1:100 in blocking solution; Santa Cruz Biotechnology Inc), MIST1 (rabbit; 1:500),⁴⁸ β -catenin (mouse; 1:500; BD Biosciences, Mississauga, ON, Canada; cat. #610153, lot#5121508), SOX9 (rabbit; 1:500; MilliporeSigma, Etobicoke, ON, Canada; cat. #AB5535, lot#3018860), insulin (mouse 1:500; Sigma; cat. #I2018; lot#092K4841), or γ H2AX (rabbit; 1:200; Santa Cruz Biotechnology Inc; cat. #sc-101696, lot#12613). Secondary antibodies used include anti-rabbit FITC (cat. #111-545-003, lot#125266) and anti-mouse FITC (cat. #115-025-003, lot#125278; 1:250; Jackson ImmunoResearch, West Grove, PA). Sections were counterstained with 4',6-diamidino-2-phenylindole and imaged using a Leica DM5500B microscope with LAS V4.4 software (Leica Microsystems Ltd, Wetzlar, Germany).

Protein Isolation and Western Blot Analyses

Protein was isolated from the middle portion of the pancreata and homogenized on ice using a Potter Elvehjem Homogenizer in extraction buffer (50 mmol/L Tris [pH 7.2], 5 mmol/L MgCl₂, 1 mmol/L CaCl₂, 1% NP-40, 0.5 mmol/L DTT, 0.5 mmol/L PMSF, 10 mmol/L NaF, 2 mmol/L NaVO₄, 150 nmol/L aprotinin, 10 μ mol/L, pepstatin, 50 μ mol/L leupeptin).⁴⁶ Homogenates were sonicated for 20 seconds on ice (level 4 Fisher Sonic Dismembrator) and centrifuged

10 minutes at 4°C at 14,000g. Supernatants were taken and frozen at -80°C until used. Isolated protein was resolved by sodium dodecylsulfate-gel electrophoresis in 10% acrylamide gels and transferred to a polyvinylidene difluoride membrane (Bio-Rad; cat. #162-0177) for Western blot analyses.⁴⁸ Primary antibodies were specific for total MAPK (tERK1/2) (rabbit 1:2500 in 5% BSA-0.1% Tween20; Cell Signaling Technology; cat. #9102, lot #26), carboxypeptidase (CPA) (rabbit 1:1000 in 5% NFDM; R&D Systems, Minneapolis, MN; cat. #AF2765, lot #wo00117071), and amylase (rabbit 1:1000 in 5% NFDM; Abcam; cat. #ab21156). After overnight incubation, blots were incubated in secondary antibody (anti-rabbit HRP, 1:10,000; Jackson Labs, Bar Harbor, ME; cat. #111-035-144) diluted in 5% NFDM for 1 hour at room temperature. Blots were developed by using Clarity Western blot ECL kit (Biorad; cat. #1705061) and visualized by using the VersaDoc system with Quantity One 1-D analysis software (Bio-Rad).

TUNEL Assay

To assess apoptosis, cryostat sections were processed using the *In Situ* Cell Death detection kit (Roche, Laval, QC, Canada; cat. #11684795910) per manufacturer's directions. Sections were counterstained with DAPI. The number of TUNEL-positive cells was quantified using 7 random fields

Table 4. Classification of ADM and PanIN Lesions 60 Days After Activation of KRAS^{G12D} and Loss of *Atrx*

Genotype	Sex	Percent of lobules determined by highest lesion grade			
		Normal	ADM	PanIN1	PanIN2
KRAS ^{LSL-G12D}	Male (7)	83.1 ± 7.8	10.8 ± 4.2	4.9 ± 3.6	1.3 ± 1.3
	Female (10)	60.1 ± 8.2	33.3 ± 6.3	6.5 ± 3.5	0 ± 0
MKA	Male (10)	81.2 ± 7.8	18.8 ± 7.8	0 ± 0	0 ± 0
	Female (6)	46.9 ± 11.9 ^a	25.2 ± 5.7	16.2 ± 8.3 ^b	11.7 ± 6.3 ^a

NOTE. (#) indicates n values. Data were assessed using 2-way ANOVA and Tukey post hoc test. These data are presented in Figure 8B.

^aDifference from all other groups ($P < .05$).

^bDifference from male MKA mice ($P < .05$).

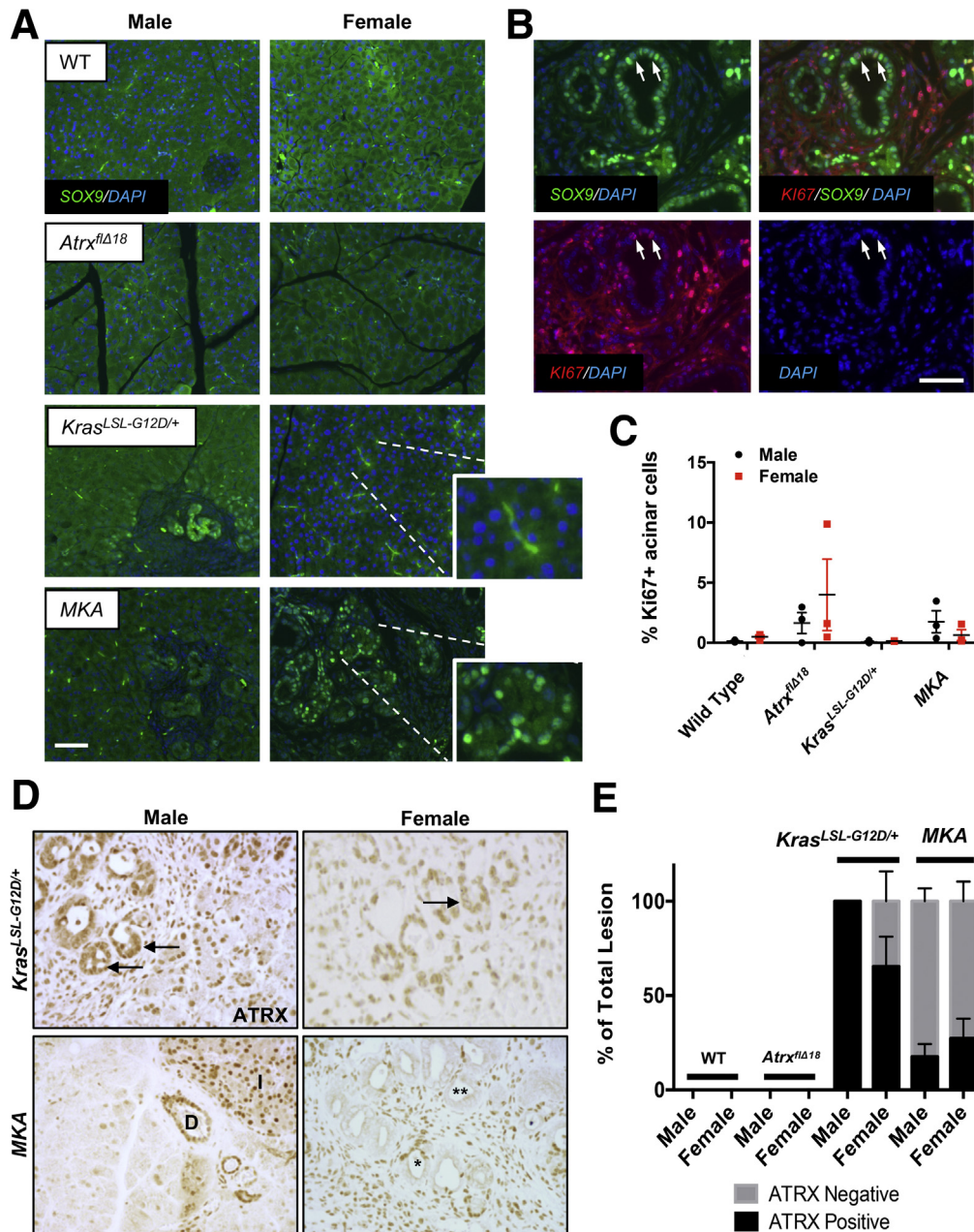


Figure 10. PanIN lesions in *Mist1*^{creERT/+} *Atrxf1Δ18* mice are derived from ATRX- acinar cells undergoing ADM. (A) Immunofluorescent images for SOX9 in male and female *Mist1*^{creERT/+} (WT), *Mist1*^{creERT/+} *Atrxf1Δ18* (*Atrxf1Δ18*), *Mist1*^{creERT/+} *Kras*^{LSL-G12D/+} (*Kras*^{LSL-G12D/+}), and MKA mice 60 days after tamoxifen treatment. *Insets* show nuclear localization of SOX9 in putative ADM in MKA mice. (B) Co-immunofluorescence of putative ADM in female MKA pancreatic tissue shows SOX9 nuclear accumulation in proliferating cells based on Ki67 accumulation (red). White arrows indicate cells expressing Ki67 and SOX9. Sections were counterstained for DAPI. Magnification bars = 50 μ m. (C) Quantification of Ki67+ acinar cells in *Mist1*^{creERT/+}, *Mist1*^{creERT/+} *Atrxf1Δ18*, *Mist1*^{creERT/+} *Kras*^{LSL-G12D/+}, and MKA mice. Bars represent mean \pm standard error. N = 3 for each group. (D) Immunohistochemistry for ATRX in putative ADM and PanINs in male and female *Mist1*^{creERT/+} *Kras*^{LSL-G12D/+} (*Kras*^{LSL-G12D/+}) and MKA mice. ATRX+ lesions are identified in *Mist1*^{creERT/+} *Kras*^{LSL-G12D/+} mice (black arrow), whereas female MKA revealed both ATRX+ (*) and ATRX- (**) cells within the PanINs. ATRX+ cells are found in ducts (D) and islets (I) of MKA males and in interstitial fibroblasts in MKA females. (E) Quantification of lesions with at least 1 ATRX+ cell (black) or no ATRX+ cells (gray) in *Mist1*^{creERT/+} (WT; n = 3 for male and female), *Mist1*^{creERT/+} *Atrxf1Δ18* (*Atrxf1Δ18*; n = 3 for male and female), *Mist1*^{creERT/+} *Kras*^{LSL-G12D/+} (*Kras*^{LSL-G12D/+}; n = 3 for male or n = 6 for female), and MKA (n = 4 for male or n = 3 for female) mice. Bars represent mean % \pm standard error.

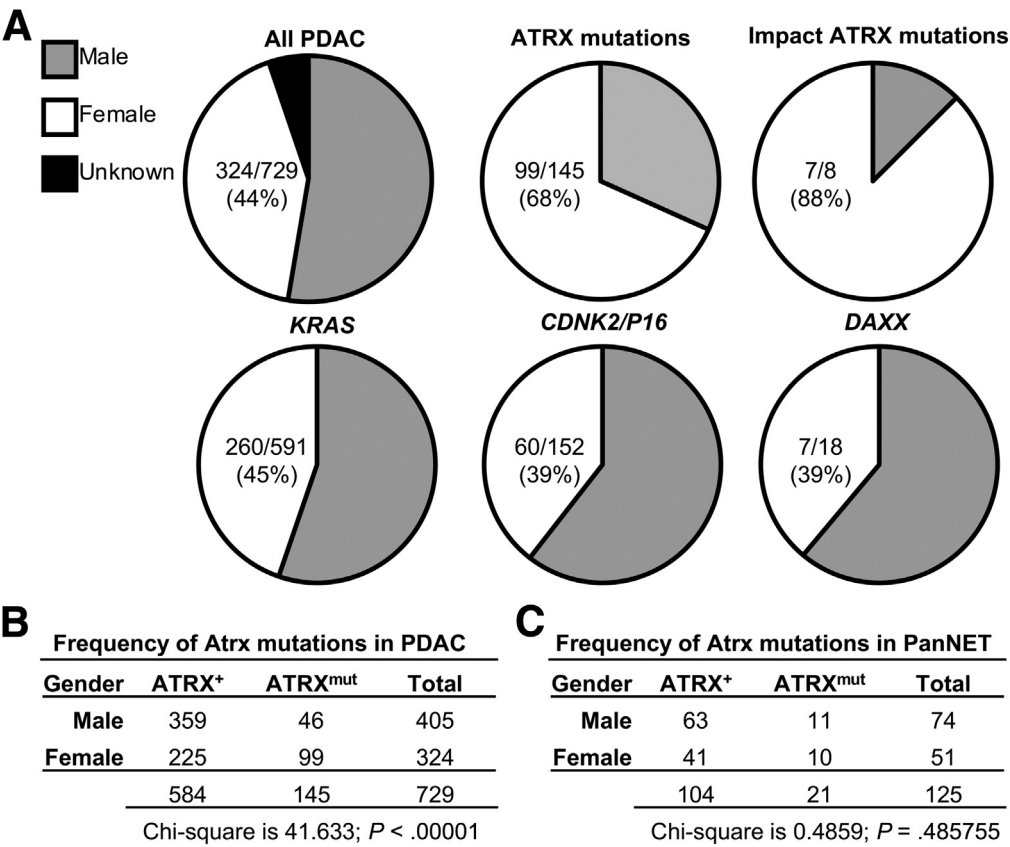


Figure 11. Mutation analysis on PDAC patients based on data from the International Cancer Genome Consortium. (A) Comparison of gender breakdown for all PDAC cases, or for mutations in *ATRX*, known driver mutations for PDAC (*KRAS*, *CDKN2/P16*), or for *DAXX*. Impact *ATRX* mutations refer to those mutations that occur with the protein coding region and are predicted to have a negative impact on protein function. (B and C) Chi-squared analyses determining if *ATRX* mutations and sex are independent variables in PDAC (B) or pancreatic neuroendocrine tumors (PNETs; C).

of view from each mouse and calculated as percentage of TUNEL-positive cells compared with DAPI counts.

Statistical Analysis

In all cases, data were analyzed for significance by using an unpaired, two-tailed *t* test or 2-way analysis of variance (ANOVA) with Tukey post hoc test. Values are depicted as means \pm standard error of the mean. Significance is considered $P < .05$.

References

1. Hingorani SR, Wang L, Multani AS, Combs C, Deramautd TB, Hruban RH, Rustgi AK, Chang S, Tuveson DA. Trp53R172H and KrasG12D cooperate to promote chromosomal instability and widely metastatic pancreatic ductal adenocarcinoma in mice. *Cancer Cell* 2005;7:469–483.
2. Zhu L, Shi G, Schmidt CM, Hruban RH, Konieczny SF. Acinar cells contribute to the molecular heterogeneity of pancreatic intraepithelial neoplasia. *Am J Pathol* 2007; 171:263–273.
3. Morris JPt, Cano DA, Sekine S, Wang SC, Hebrok M. Beta-catenin blocks Kras-dependent reprogramming of acini into pancreatic cancer precursor lesions in mice. *J Clin Invest* 2010;120:508–520.
4. Kopp JL, von Figura G, Mayes E, Liu FF, Dubois CL, Morris JP, Pan FC, Akiyama H, Wright CV, Jensen K,

Hebrok M, Sander M. Identification of Sox9-dependent acinar-to-ductal reprogramming as the principal mechanism for initiation of pancreatic ductal adenocarcinoma. *Cancer Cell* 2012;22:737–750.

5. Shi G, Drenzo D, Qu C, Barney D, Miley D, Konieczny SF. Maintenance of acinar cell organization is critical to preventing Kras-induced acinar-ductal metaplasia. *Oncogene* 2013;32: 1950–1958.
6. Bardeesy N, Aguirre AJ, Chu GC, Cheng KH, Lopez LV, Hezel AF, Feng B, Brennan C, Weissleder R, Mahmood U, Hanahan D, Redston MS, Chin L, Depinho RA. Both p16(Ink4a) and the p19(Arf)-p53 pathway constrain progression of pancreatic adenocarcinoma in the mouse. *Proc Natl Acad Sci U S A* 2006; 103:5947–5952.
7. De La OJ, Emerson LL, Goodman JL, Froebe SC, Illum BE, Curtis AB, Murtaugh LC. Notch and Kras reprogram pancreatic acinar cells to ductal intraepithelial neoplasia. *Proc Natl Acad Sci U S A* 2008; 105:18907–18912.
8. Bailey P, Chang DK, Nones K, Johns AL, Patch AM, Gingras MC, Miller DK, Christ AN, Bruxner TJ, Quinn MC, Nourse C, Murtaugh LC, Harliwong I, Idrisoglu S, Manning S, Nourbakhsh E, Wani S, Fink L, Holmes O, Chin V, Anderson MJ, Kazakoff S, Leonard C, Newell F, Waddell N, Wood S, Xu Q, Wilson PJ, Cloonan N, Kassahn KS, Taylor D, Quek K, Robertson A, Pantano L,

- Mincarelli L, Sanchez LN, Evers L, Wu J, Pinese M, Cowley MJ, Jones MD, Colvin EK, Nagrial AM, Humphrey ES, Chantrill LA, Mawson A, Humphris J, Chou A, Pajic M, Scarlett CJ, Pinho AV, Giry-Laterriere M, Rooman I, Samra JS, Kench JG, Lovell JA, Merrett ND, Toon CW, Epari K, Nguyen NQ, Barbour A, Zeps N, Moran-Jones K, Jamieson NB, Graham JS, Duthie F, Oien K, Hair J, Grutzmann R, Maitra A, Iacobuzio-Donahue CA, Wolfgang CL, Morgan RA, Lawlor RT, Corbo V, Bassi C, Rusev B, Capelli P, Salvia R, Tortora G, Mukhopadhyay D, Petersen GM, Australian Pancreatic Cancer Genome, Munzy DM, Fisher WE, Karim SA, Eshleman JR, Hruban RH, Pilarsky C, Morton JP, Sansom OJ, Scarpa A, Musgrove EA, Bailey UH, Hofmann O, Sutherland RL, Wheeler DA, Gill AJ, Gibbs RA, Pearson JV, Waddell N, Biankin AV, Grimmond SM. Genomic analyses identify molecular subtypes of pancreatic cancer. *Nature* 2016; 531:47–52.
9. von Figura G, Fukuda A, Roy N, Liku ME, Morris JP, Kim GE, Russ HA, Firpo MA, Mulvihill SJ, Dawson DW, Ferrer J, Mueller WF, Busch A, Hertel KJ, Hebrok M. The chromatin regulator Brg1 suppresses formation of intra-ductal papillary mucinous neoplasm and pancreatic ductal adenocarcinoma. *Nat Cell Biol* 2014;16:255–267.
 10. Bednar F, Schofield HK, Collins MA, Yan W, Zhang Y, Shyam N, Eberle JA, Almada LL, Olive KP, Bardeesy N, Fernandez-Zapico ME, Nakada D, Simeone DM, Morrison SJ, Pasca di Magliano M. Bmi1 is required for the initiation of pancreatic cancer through an Ink4a-independent mechanism. *Carcinogenesis* 2015; 36:730–738.
 11. Lewis PW, Elsaesser SJ, Noh KM, Stadler SC, Allis CD. Daxx is an H3.3-specific histone chaperone and co-operates with ATRX in replication-independent chromatin assembly at telomeres. *Proc Natl Acad Sci U S A* 2010;107:14075–14080.
 12. Goldberg AD, Banaszynski LA, Noh KM, Lewis PW, Elsaesser SJ, Stadler S, Dewell S, Law M, Guo X, Li X, Wen D, Chapgier A, DeKolver RC, Miller JC, Lee YL, Boydston EA, Holmes MC, Gregory PD, Grealley JM, Rafii S, Yang C, Scambler PJ, Garrick D, Gibbons RJ, Higgs DR, Cristea IM, Urnov FD, Zheng D, Allis CD. Distinct factors control histone variant H3.3 localization at specific genomic regions. *Cell* 2010;140:678–691.
 13. Lovejoy CA, Li W, Reisenweber S, Thongthip S, Bruno J, de Lange T, De S, Petrini JH, Sung PA, Jasin M, Rosenbluh J, Zwang Y, Weir BA, Hatton C, Ivanova E, Macconail L, Hanna M, Hahn WC, Lue NF, Reddel RR, Jiao Y, Kinzler K, Vogelstein B, Papadopoulos N, Meeker AK; Consortium ALTSC. Loss of ATRX, genome instability, and an altered DNA damage response are hallmarks of the alternative lengthening of telomeres pathway. *PLoS Genet* 2012;8:e1002772.
 14. Clynes D, Jelinska C, Xella B, Ayyub H, Taylor S, Mitson M, Bachrati CZ, Higgs DR, Gibbons RJ. ATRX dysfunction induces replication defects in primary mouse cells. *PLoS One* 2014;9:e92915.
 15. Levy MA, Kernohan KD, Jiang Y, Berube NG. ATRX promotes gene expression by facilitating transcriptional elongation through guanine-rich coding regions. *Hum Mol Genet* 2015;24:1824–1835.
 16. Law MJ, Lower KM, Voon HP, Hughes JR, Garrick D, Viprakasit V, Mitson M, De Gobbi M, Marra M, Morris A, Abbott A, Wilder SP, Taylor S, Santos GM, Cross J, Ayyub H, Jones S, Ragoussis J, Rhodes D, Dunham I, Higgs DR, Gibbons RJ. ATR-X syndrome protein targets tandem repeats and influences allele-specific expression in a size-dependent manner. *Cell* 2010;143:367–378.
 17. Garrick D, Sharpe JA, Arkell R, Dobbie L, Smith AJ, Wood WG, Higgs DR, Gibbons RJ. Loss of Atrx affects trophoblast development and the pattern of X-inactivation in extraembryonic tissues. *PLoS Genet* 2006;2:e58.
 18. Gibbons RJ, Picketts DJ, Villard L, Higgs DR. Mutations in a putative global transcriptional regulator cause X-linked mental retardation with alpha-thalassemia (ATR-X syndrome). *Cell* 1995;80:837–845.
 19. Jiao Y, Shi C, Edil BH, de Wilde RF, Klimstra DS, Maitra A, Schlick RD, Tang LH, Wolfgang CL, Choti MA, Velculescu VE, Diaz LA, Vogelstein B, Kinzler KW, Hruban RH, Papadopoulos N. DAXX/ATRX, MEN1, and mTOR pathway genes are frequently altered in pancreatic neuroendocrine tumors. *Science* 2011;331:1199–1203.
 20. Singhi AD, Liu TC, Roncalioli JL, Cao D, Zeh HJ, Zureikat AH, Tsung A, Marsh JW, Lee KK, Hogg ME, Bahary N, Brand RE, McGrath KM, Slivka A, Cressman KL, Fuhrer K, O'Sullivan RJ. Alternative lengthening of telomeres and loss of DAXX/ATRX expression predicts metastatic disease and poor survival in patients with pancreatic neuroendocrine tumors. *Clin Cancer Res* 2017;23:600–609.
 21. Kannan K, Inagaki A, Silber J, Gorovets D, Zhang J, Kastnerhuber ER, Heguy A, Petrini JH, Chan TA, Huse JT. Whole-exome sequencing identifies ATRX mutation as a key molecular determinant in lower-grade glioma. *Oncotarget* 2012;3:1194–1203.
 22. Koschmann C, Lowenstein PR, Castro MG. ATRX mutations and glioblastoma: impaired DNA damage repair, alternative lengthening of telomeres, and genetic instability. *Mol Cell Oncol* 2016;3:e1167158.
 23. Berube NG, Mangelsdorf M, Jagla M, Vanderluit J, Garrick D, Gibbons RJ, Higgs DR, Slack RS, Picketts DJ. The chromatin-remodeling protein ATRX is critical for neuronal survival during corticogenesis. *J Clin Invest* 2005;115:258–267.
 24. Johnson CL, Peat JM, Volante SN, Wang R, McLean CA, Pin CL. Activation of protein kinase C delta leads to increased pancreatic acinar cell de-differentiation in the absence of MIST1. *J Pathol* 2012;228:351–365.
 25. Shi G, Zhu L, Sun Y, Bettencourt R, Damsz B, Hruban RH, Konieczny SF. Loss of the acinar-restricted transcription factor Mist1 accelerates Kras-induced pancreatic intraepithelial neoplasia. *Gastroenterology* 2009;136:1368–1378.
 26. Garrick D, Samara V, McDowell TL, Smith AJ, Dobbie L, Higgs DR, Gibbons RJ. A conserved truncated isoform of the ATR-X syndrome protein lacking the SWI/SNF-homology domain. *Gene* 2004;326:23–34.

27. Ritchie K, Seah C, Moulin J, Isaac C, Dick F, Berube NG. Loss of ATRX leads to chromosome cohesion and congression defects. *J Cell Biol* 2008;180:315–324.
28. Prevot PP, Simion A, Grimont A, Colletti M, Khalaileh A, Van den Steen G, Sempoux C, Xu X, Roelants V, Hald J, Bertrand L, Heimberg H, Konieczny SF, Dor Y, Lemaigre FP, Jacquemin P. Role of the ductal transcription factors HNF6 and Sox9 in pancreatic acinar-to-ductal metaplasia. *Gut* 2012;61:1723–1732.
29. Martinelli P, Madriles F, Canamero M, Pau EC, Pozo ND, Guerra C, Real FX. The acinar regulator Gata6 suppresses KrasG12V-driven pancreatic tumorigenesis in mice. *Gut* 2016;65:476–486.
30. Ledda-Columbano GM, Perra A, Pibiri M, Molotzu F, Columbano A. Induction of pancreatic acinar cell proliferation by thyroid hormone. *J Endocrinol* 2005;185:393–399.
31. Hess DA, Humphrey SE, Ishibashi J, Damsz B, Lee AH, Glimcher LH, Konieczny SF. Extensive pancreas regeneration following acinar-specific disruption of Xbp1 in mice. *Gastroenterology* 2011;141:1463–1472.
32. Roy N, Takeuchi KK, Ruggeri JM, Bailey P, Chang D, Li J, Leonhardt L, Puri S, Hoffman MT, Gao S, Halbrook CJ, Song Y, Ljungman M, Malik S, Wright CV, Dawson DW, Biankin AV, Hebros M, Crawford HC. PDX1 dynamically regulates pancreatic ductal adenocarcinoma initiation and maintenance. *Genes Dev* 2016;30:2669–2683.
33. Mallen-St Clair J, Soydaner-Azeloglu R, Lee KE, Taylor L, Livanos A, Pylayeva-Gupta Y, Miller G, Margueron R, Reinberg D, Bar-Sagi D. EZH2 couples pancreatic regeneration to neoplastic progression. *Genes Dev* 2012;26:439–444.
34. Guerra C, Schuhmacher AJ, Canamero M, Grippo PJ, Verdaguer L, Perez-Gallego L, Dubus P, Sandgren EP, Barbacid M. Chronic pancreatitis is essential for induction of pancreatic ductal adenocarcinoma by K-Ras oncogenes in adult mice. *Cancer Cell* 2007;11:291–302.
35. de Wilde RF, Heaphy CM, Maitra A, Meeker AK, Edil BH, Wolfgang CL, Ellison TA, Schulick RD, Molenaar IQ, Valk GD, Vriens MR, Borel Rinkes IH, Offerhaus GJ, Hruban RH, Matsukuma KE. Loss of ATRX or DAXX expression and concomitant acquisition of the alternative lengthening of telomeres phenotype are late events in a small subset of MEN-1 syndrome pancreatic neuroendocrine tumors. *Mod Pathol* 2012;25:1033–1039.
36. Heaphy CM, de Wilde RF, Jiao Y, Klein AP, Edil BH, Shi C, Bettgeowda C, Rodriguez FJ, Eberhart CG, Hebbar S, Offerhaus GJ, McLendon R, Rasheed BA, He Y, Yan H, Bigner DD, Oba-Shinjo SM, Marie SK, Riggins GJ, Kinzler KW, Vogelstein B, Hruban RH, Maitra A, Papadopoulos N, Meeker AK. Altered telomeres in tumors with ATRX and DAXX mutations. *Science* 2011;333:425.
37. van Heek T, Rader AE, Offerhaus GJ, McCarthy DM, Goggins M, Hruban RH, Wilentz RE. K-ras, p53, and DPC4 (MAD4) alterations in fine-needle aspirates of the pancreas: a molecular panel correlates with and supplements cytologic diagnosis. *Am J Clin Pathol* 2002;117:755–765.
38. Cardoso C, Timsit S, Villard L, Khrestchatsky M, Fontes M, Colleaux L. Specific interaction between the XNP/ATR-X gene product and the SET domain of the human EZH2 protein. *Hum Mol Genet* 1998;7:679–684.
39. Nussler NC, Reinbacher K, Shanny N, Schirmeier A, Glanemann M, Neuhaus P, Nussler AK, Kirschner M. Sex-specific differences in the expression levels of estrogen receptor subtypes in colorectal cancer. *Gend Med* 2008;5:209–217.
40. Daniluk J, Liu Y, Deng D, Chu J, Huang H, Gaiser S, Cruz-Monserate Z, Wang H, Ji B, Logsdon CD. An NF-kappaB pathway-mediated positive feedback loop amplifies Ras activity to pathological levels in mice. *J Clin Invest* 2012;122:1519–1528.
41. Baumgart S, Chen NM, Siveke JT, Konig A, Zhang JS, Singh SK, Wolf E, Bartkuhn M, Esposito I, Hessmann E, Reinecke J, Nikorowitsch J, Brunner M, Singh G, Fernandez-Zapico ME, Smyrk T, Bamlet WR, Eilers M, Neesse A, Gress TM, Billadeu DD, Tuveson D, Urrutia R, Ellenrieder V. Inflammation-induced NFATc1-STAT3 transcription complex promotes pancreatic cancer initiation by KrasG12D. *Cancer Discov* 2014;4:688–701.
42. Akiyama H, Stadler HS, Martin JF, Ishii TM, Beachy PA, Nakamura T, de Crombrughe B. Misexpression of Sox9 in mouse limb bud mesenchyme induces polydactyly and rescues hypodactyly mice. *Matrix Biology* 2007;26:224–233.
43. Jeselsohn R, Cornwell M, Pun M, Buchwalter G, Nguyen M, Bango C, Huang Y, Kuang Y, Paweletz C, Fu X, Nardone A, De Angelis C, Detre S, Dodson A, Mohammed H, Carroll JS, Bowden M, Rao P, Long HW, Li F, Dowsett M, Schiff R, Brown M. Embryonic transcription factor SOX9 drives breast cancer endocrine resistance. *PNAS* 2017;114:E4482–E4491.
44. Karki A, Humphrey SE, Steele RE, Karki A, Humphrey SE, Steele RE, Hess DA, Taparowsky EJ, Konieczny SF. Silencing Mist1 gene expression is essential for recovery from acute pancreatitis. *PLoS One* 2015;10:e0145724.
45. Jackson EL, Willis N, Mercer K, Bronson RT, Crowley D, Montoya R, Jacks T, Tuveson DA. Analysis of lung tumor initiation and progression using conditional expression of K-ras. *Genes Develop* 2001;15:3243–3248.
46. Fazio EN, Young CC, Toma J, Levy M, Berger KR, Johnson CL, Mehmood R, Swan P, Chu A, Cregan SP, Dilworth FJ, Howlett CJ, Pin CL. Activating transcription factor 3 promotes loss of the acinar cell phenotype in response to cerulein-induced pancreatitis in mice. *Mol Biol Cell* 2017;28:2347–2359.
47. Schindelin J, Arganda-Carreras I, Frise E, Kaynig V, Longair M, Pietzsch T, Preibisch S, Rueden C, Saalfeld S, Schmid B, Tinevez JY, White DJ, Hartenstein V, Eliceiri K, Tomancak P, Cardona A. Fiji: an open-source platform for biological-image analysis. *Nat Methods* 2012;9:676–682.
48. Pin CL, Bonvissuto AC, Konieczny SF. Mist1 expression is a common link among serous exocrine cells exhibiting regulated exocytosis. *Anat Rec* 2000;259:157–167.

Received February 28, 2018. Accepted September 6, 2018.

Correspondence

Address correspondence to: Christopher Pin, PhD, Department of Paediatrics, University of Western Ontario, Children's Health Research Institute, 5th Floor, Victoria Research Laboratories, London, Ontario, Canada N6C 2V5. e-mail: cpin@uwo.ca; fax: (519) 685-8186.

Author contributions

CY: acquisition of data, analysis and interpretation of data, drafting of the manuscript; RB: acquisition of data, analysis and interpretation of data; CH: analysis and interpretation of data; TH: acquisition of data; JH: acquisition of data; DH: material support; RG: material support;

HC: acquisition of data, analysis and interpretation of data, critical revision of the manuscript for important intellectual content; AB: critical revision of the manuscript for important intellectual content; CP: study concept and design, drafting of the manuscript, critical revision of the manuscript for important intellectual content, obtained funding, study supervision.

Conflicts of interest

The authors disclose no conflicts.

Funding

Funding was provided to C.P. by the Rob Lutterman Memorial Foundation and Cancer Research Society of Canada. C.Y. was funded by a Canadian Graduate Scholarship. R.B. received a Canadian Association of Gastroenterology summer scholarship.